



SEMICONDUCTOR RADIATION DETECTOR MATERIALS: FACTS VERSUS FICTION

Eugene E. Haller
University of California and
LBNL, Berkeley, CA 94720

LBNL Instrumentation Colloquium, 2/15/2006



General References



- "Radiation Detection and Measurement," (3rd edition), G.F. Knoll (J. Wiley & Sons, 2000); pp. 353-503.
- "Semiconductor Detector Systems," H. Spieler (Oxford Univ. Press, 2005).
- "Nuclear Radiation Detector Materials," eds. E.E. Haller, H.W. Kraner and W.A. Higginbotham, Mat. Res. Soc. Proc. Vol. 16 (North Holland, 1983).
- "Detector Materials: Germanium and Silicon," E.E. Haller, IEEE Trans. Nucl. Sci. NS-29, No. 3, 1109-18 (1982).
- "Nuclear Radiation Detectors," E.E. Haller and F.S. Goulding, in Handbook on Semiconductors, 2nd edition, ed. C. Hilsum (Elsevier North Holland, 1993), pp. 937-63.



Nuclear Instruments and Methods in Physics Research A **531** (2004)18 –37

Compound semiconductor radiation detectors

Alan Owens*, A.Peacock

Abstract

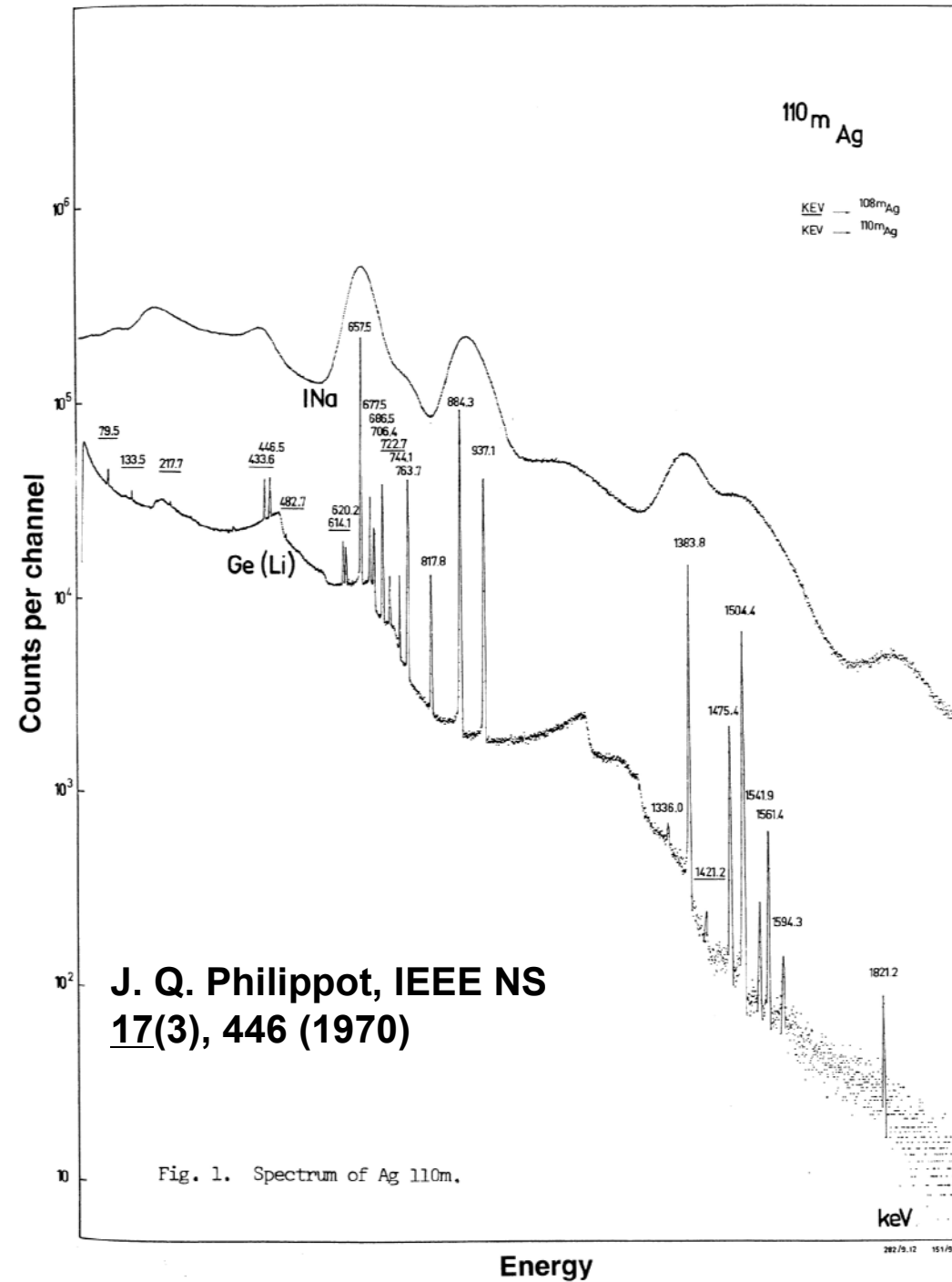
We discuss the potential benefits of using compound semiconductors for the detection of X-and g ray radiation. While Si and Ge have become detection standards for energy dispersive spectroscopy in the laboratory, their use for an increasing range of applications is becoming marginalized by one or more of their physical limitations; namely the need for ancillary cooling systems or bulky cryogenics, their modest stopping powers and radiation intolerance. **Compound semiconductors encompass such a wide range of physical properties that it is technically feasible to engineer a material to any application.** Wide band-gap compounds offer the ability to operate in a wide range of thermal and radiation environments, whilst still maintaining sub-keV spectral resolution at hard X-ray wavelengths. Narrow band-gap materials, on the other hand, offer the potential of exceeding the spectral resolution of both Si and Ge, by as much as a factor of 3...

FICTION



Topics to be discussed

- The Ionization Chamber
- Semiconductor Properties
- Interaction of Radiation with Semiconductors
- P-N-Junctions
- Detector Materials: Ge, Si, (GaAs)
- Room Temperature and High Z Materials: CdTe, CdZnTe, HgI₂, GaAs, AlSb
- Conclusions

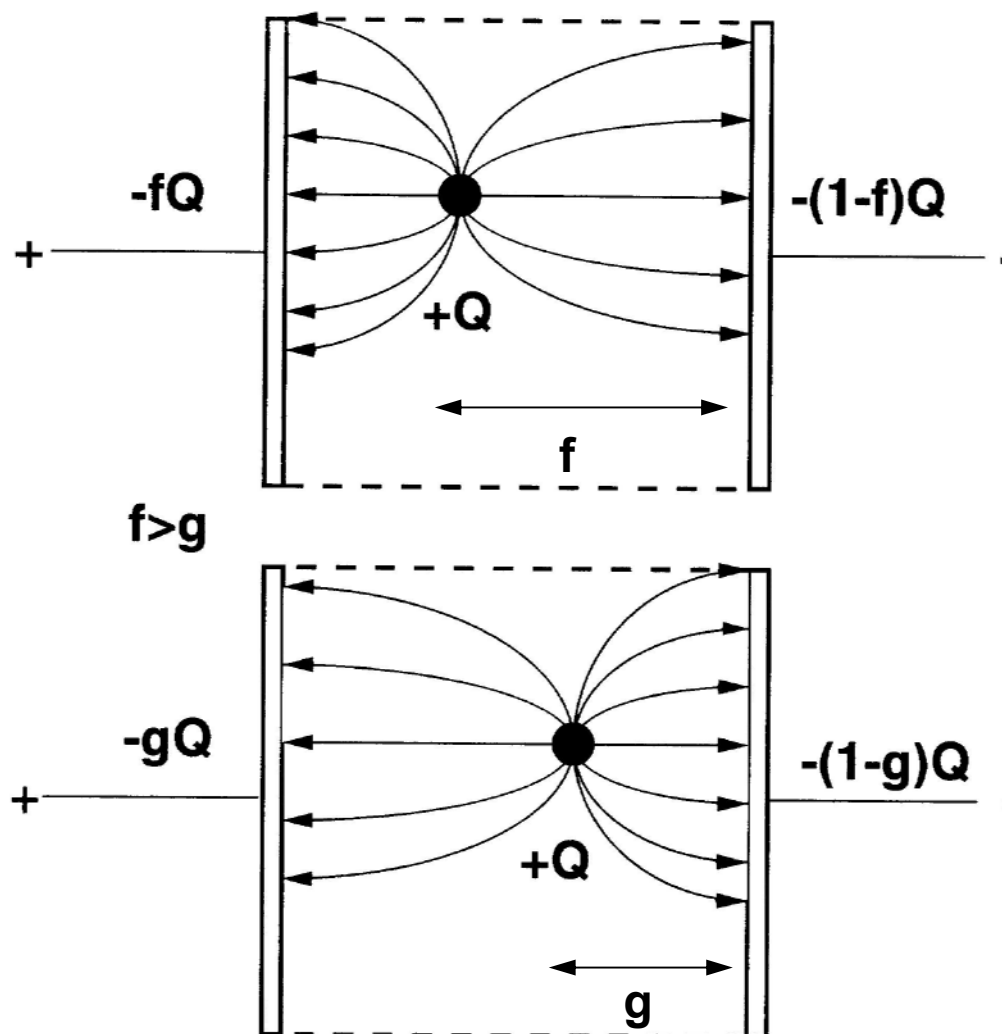


2/15/2006

E. E. Haller 5



The Ionization Chamber: Displacement Current and Charge Collection



Applies to:

- reverse biased p-n or p-i-n junction,
- resistive detectors,
- gas ionization chambers,
- proportional counters, etc.



The Ionization Chamber: Operating Principle

The field lines of a charge in volume V end on the electrodes and "influence" an electric charge. The relative quantities of charge influenced on each electrode depends only on the geometry. When the charge moves (in an externally applied field), the relative quantities of influenced charge change, forming a displacement current. When the charge stops moving, the displacement current stops flowing. Charge may stop flowing because it gets "trapped" at a defect center or gets "collected" at a contact. In a typical p-n junction, charge ideally flows to one of the electrodes. In a resistive detector, charge arriving at one electrode may lead to the injection of a new charge at the opposite electrode.

We define the "photoconductive" gain: $G = \frac{\bar{\ell}}{L}$

$\bar{\ell}$ = average distance traveled by a free charge
 L = inter electrode distance

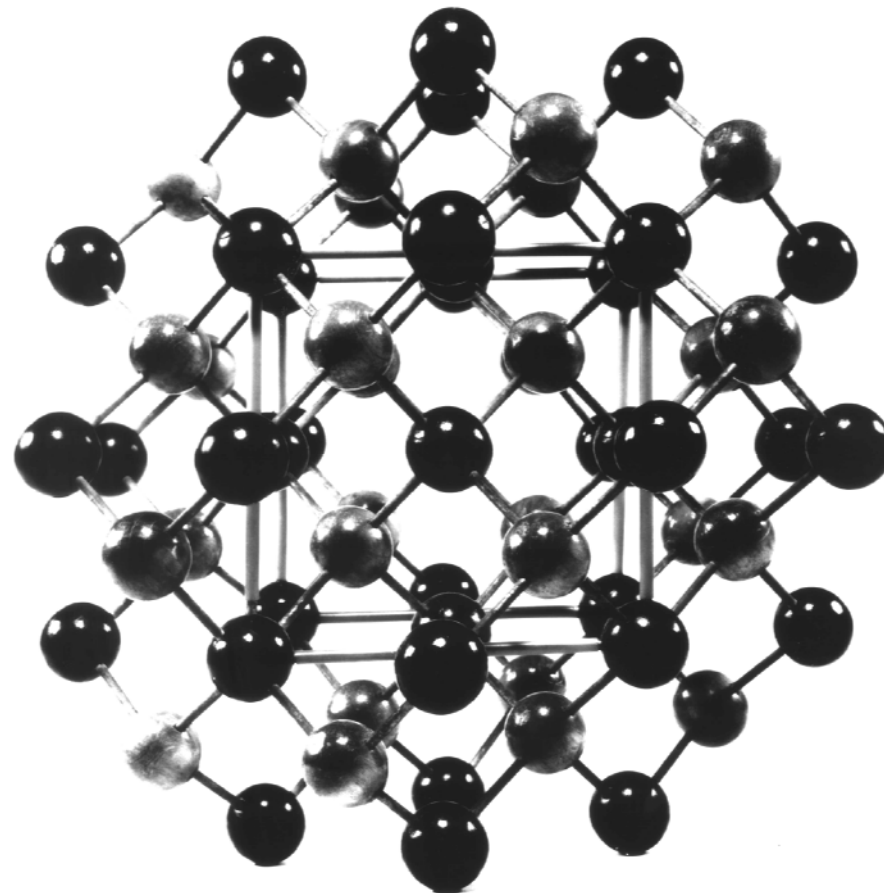
Note: For a high resolution detector, a fixed, constant gain is required (for p-n junctions: $G = 1.00$)



SEMICONDUCTOR PROPERTIES

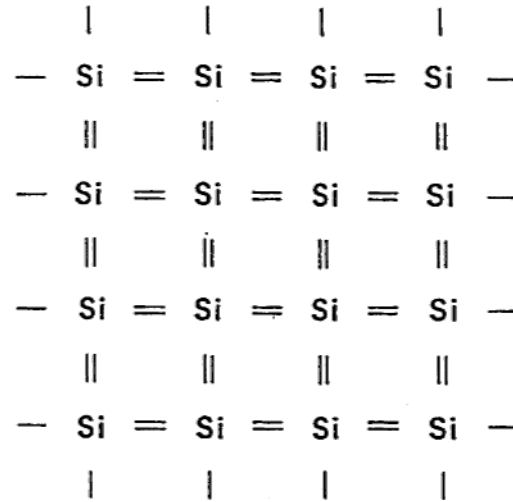


Diamond Crystal Lattice: $[100]$ Direction

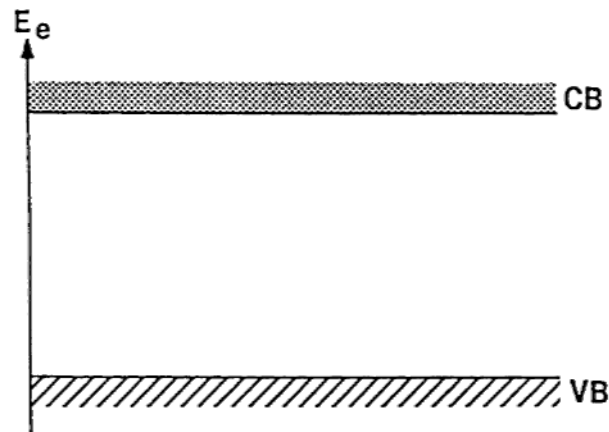




Silicon



- A) Real space structure,
[100] projection
(The sign = represents the two
electrons in each bond.)



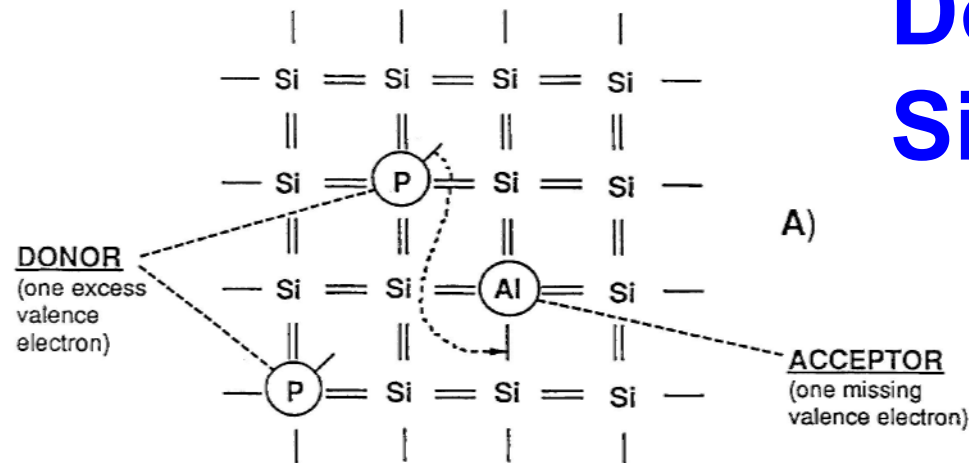
- B) Electronic band structure
(CB = conduction band,
VB = valence band)

PURE AND PERFECT CRYSTAL AT T=0 K

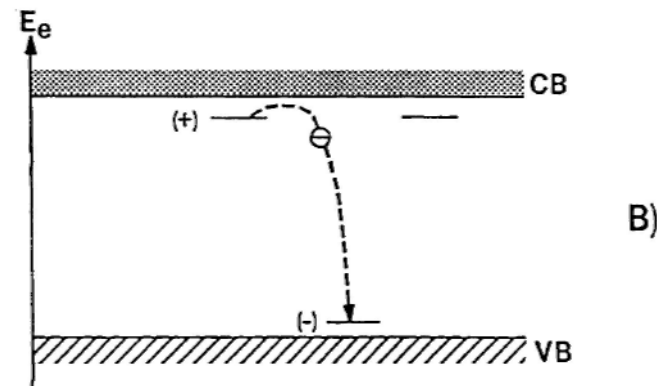
XBL 8111-12691



Doped Silicon



Donor doping (e.g., phosphorus on Si sites) provides extra electrons which can move into the conduction band or compensate an acceptor;



P & Al DOPED CRYSTAL AT T=0 K

XBL 8111-12690

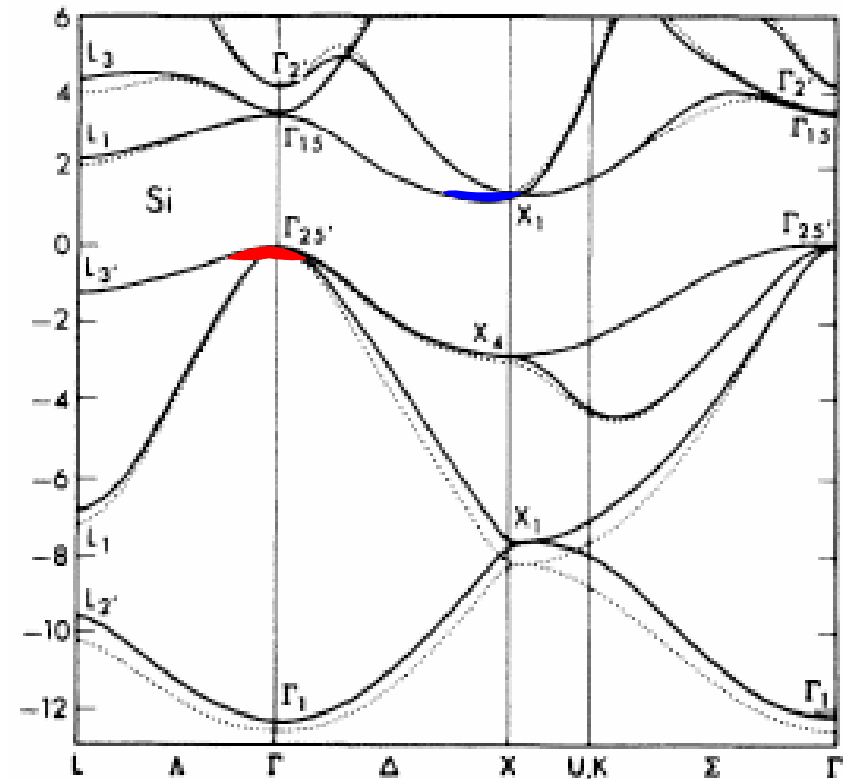
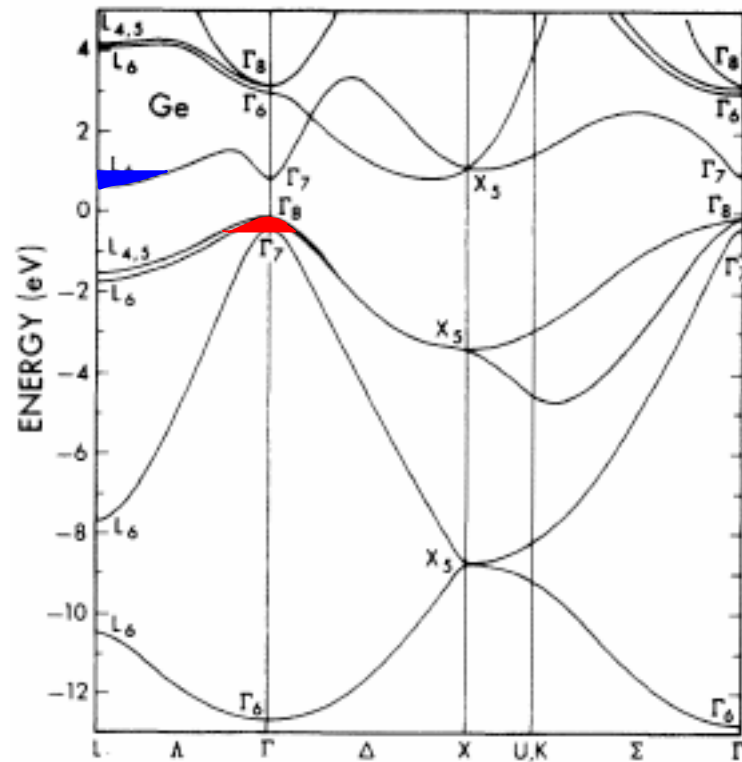
Acceptor doping (e.g., aluminum on Si sites) creates holes which can move into the valence band or compensate a donor



Bandstructures of Ge and Si



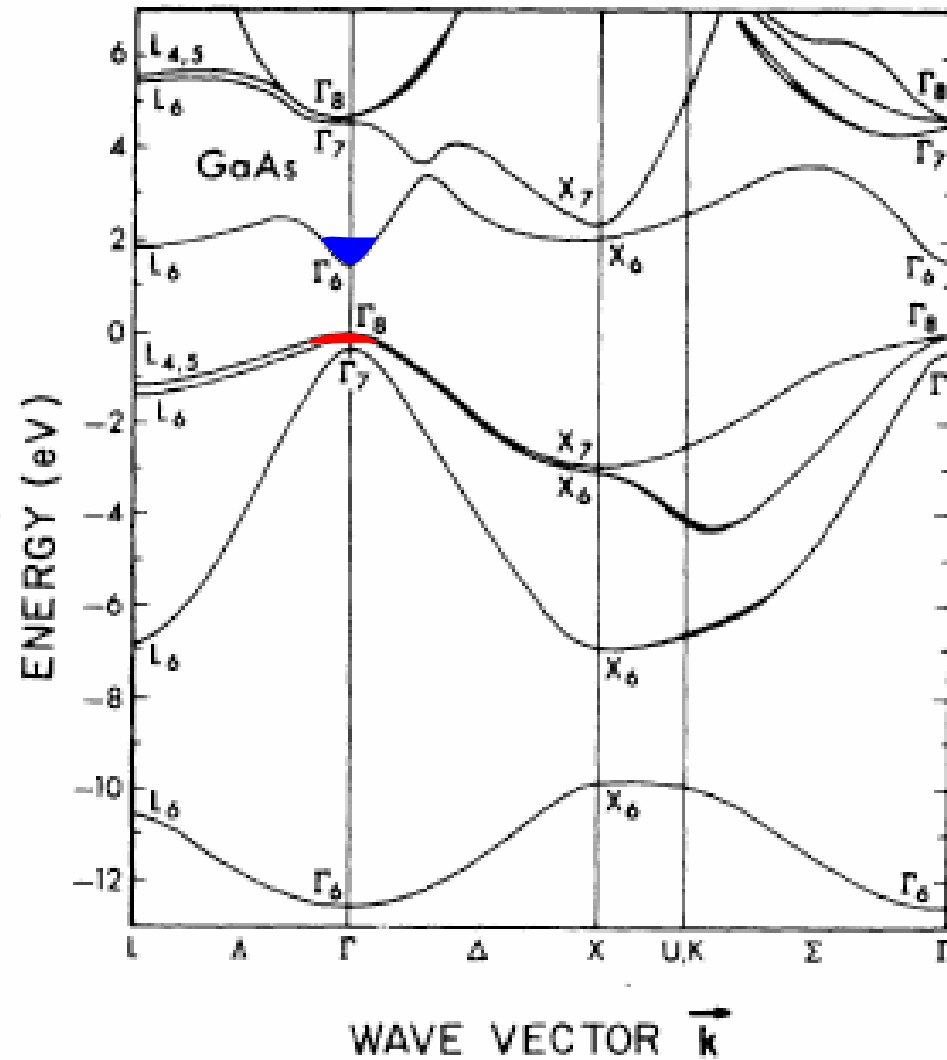
are *indirect*



\vec{k} -vector



GaAs Bandstructure is *direct*





Temperature Effects



Radiation detector performance is affected by temperature in several ways. Two important ones are:

A. Generation of free electrons and holes by **thermal ionization** across the bandgap. This affects the bias current I (also called "leakage" or "dark" current) through the detector.

This current is a source of electrical noise, in its simplest case "shot" noise ($\overline{I^2}df = 2eIdf$; e = charge of the electron, f = frequency)

B. **Trapping and de-trapping** of the free charge carriers at defect or doping related energy levels in the bandgap.



A. Free Carrier Concentration



At finite temperatures a very small number of bonds in a crystal is broken. For each broken bond there exists a mobile electron and a mobile hole. The concentration of these electrons and holes is called *intrinsic carrier concentration* n_i :

$$n_i^2 = N_c N_v \exp (-E_{\text{gap}}/k_B T)$$

N_c = conduction band effective density of states

N_v = valence band effective density of states

k_B = Boltzmann's constant = 8.65×10^{-5} eV/K

E_{gap} = energy gap (Si: 1.1 eV, Ge: 0.7 eV, GaAs = 1.42 eV, CdTe: 1.47 eV, HgI₂: 2.13 eV, AlSb: 1.58 eV)

$$n_i (\text{Si}, 300\text{K}) = 2 \times 10^{10} \text{ cm}^{-3}$$

$$n_i (\text{Ge}, 300\text{K}) = 3 \times 10^{13} \text{ cm}^{-3}$$

$$n_i (\text{GaAs}, 300\text{K}) = 10^7 \text{ cm}^{-3}$$



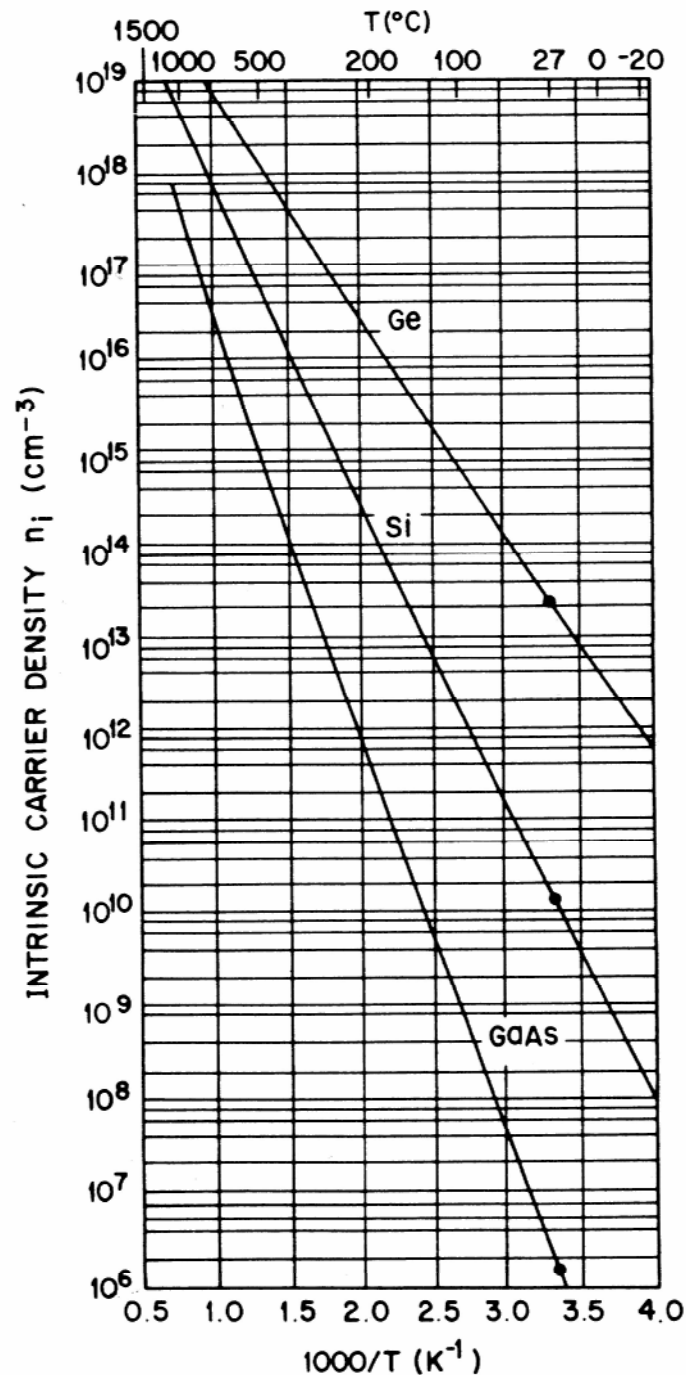
Thermal Carrier Generation



The thermal generation of electrons and holes gives rise to the reverse (also called "leakage" or "dark") current. This current constitutes a source of electronic noise.

Consequences

- Because of the small bandgap, Ge diodes must be cooled in order to achieve sufficiently low reverse currents.
- Si diodes have to be cooled only for high resolution applications.
- CdTe, CdZnTe, GaAs, AlSb and HgI₂ do not require cooling.



Arrhenius plot of the intrinsic carrier concentration of some major semiconductors



Semiconductor Band Gaps



Band-gap energy (eV)	Elemental group IVB	Binary IV–IV compounds	Binary III–V compounds	Binary II–VI compounds	Binary IV–VI compounds	Binary <i>n</i> -VIIB compounds	Ternary compounds
0.00–0.25	Sn		InSb	HgTe			HgCdTe
0.25–0.50			InAs	HgSe	PbSe, PbS, PbTe		
0.50–0.75	Ge		GaSb				InGaAs
0.75–1.00		SiGe					
1.10–1.25	Si						
1.25–1.50			GaAs, InP	CdTe			AlInAs
1.50–1.75			AlSb	CdSe			AlGaAs
1.75–2.00			BP, InN				CdZnTe, CdZnSe, InAlP
2.10–2.25		SiC	AlAs	HgS		HgI ₂	CdMnTe
2.25–2.50			GaP, AlP	ZnTe, CdS		PbI ₂	
2.50–2.75				ZnSe		TlBr	TlBrI, InAlP, TlPbI ₃
2.75–3.00				MnSe			
3.10–3.25				MnTe			
3.25–3.50			GaN	MgTe, MnS			
3.50–3.75				MgSe, ZnS			
3.75–4.00							
4.10–4.25							
4.25–4.50				MgS			
4.50–4.75							
4.75–5.00							
5.10–5.25	C						
5.25–5.50							
5.50–5.75							
5.75–6.00			BN				
6.10–6.25			AlN				
6.25–6.50							
6.50–6.75							
6.75–7.00							

Note: Compounds are listed in order of increasing band-gap energy.



B. Charge Trapping



Electrons and holes are created in ionization events caused by radiation. In order to be detected they have to traverse the detector crystal all the way to their respective electrodes. On the way they encounter impurities, some of which are charged. Trapping and release from such ionized impurities is described as follows:

emission rate e (per level) of a carrier to the nearest band:

$$\underline{e = \sigma \langle v \rangle N_{\text{band}} \exp(-E/k_B T)}$$

with

σ = carrier capture cross-section (cm^2)

$\langle v \rangle$ = average thermal velocity = $(3kT/m^*)^{1/2}$

N_{band} = effective density of states
 $= 2 (2\pi m^* kT/h^2)^{3/2}$

k_B = $8.65 \times 10^{-5} \text{ eV/K}$

E = binding energy of a particular level



B. Charge Trapping (cont.)

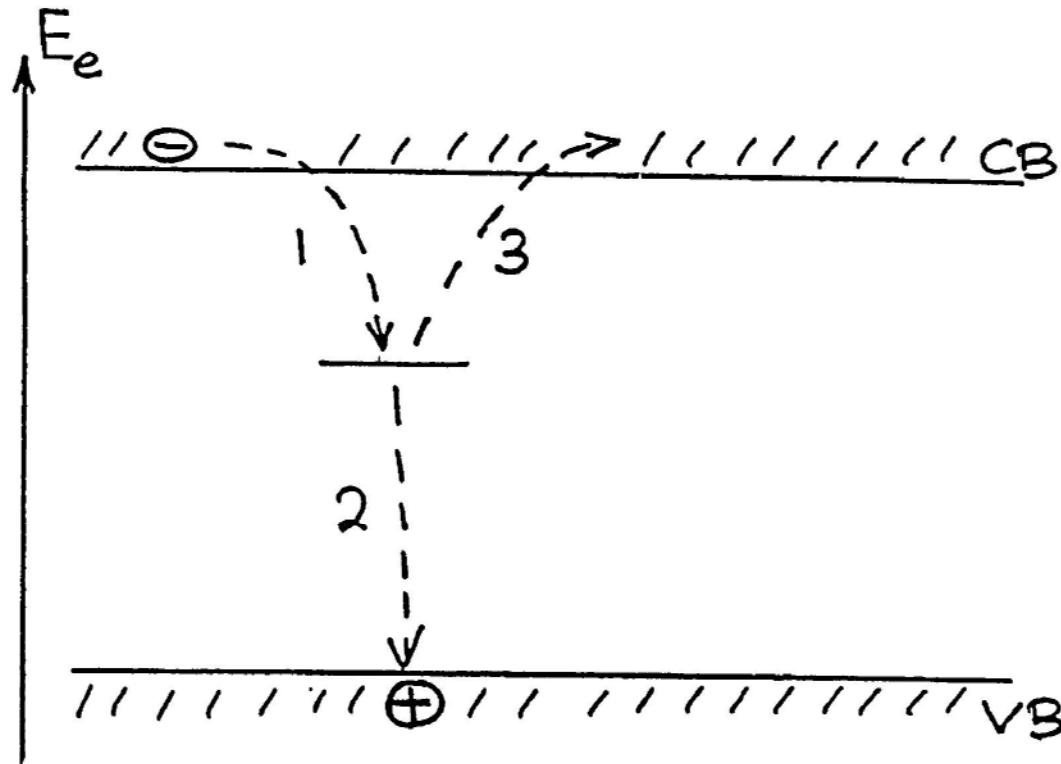


Shallow dopant levels in Si ($E \sim 45$ meV) or Ge ($E \sim 10$ meV) do not trap charge for any significant length of time at temperatures above 77 K (liquid nitrogen).

However, already very small concentrations of *deep levels* ($E > 100$ meV) trap charge effectively and do not release it within the collection time. The fluctuations in this charge loss lead to asymmetric peaks in the energy spectrum.



Deep Levels \longleftrightarrow Trapping



1: trapping of an electron on a deep level.

either 2: recombination of the trapped electron with a free hole.

or 3: detrapping after a time t .



The Origin of Deep Level Traps

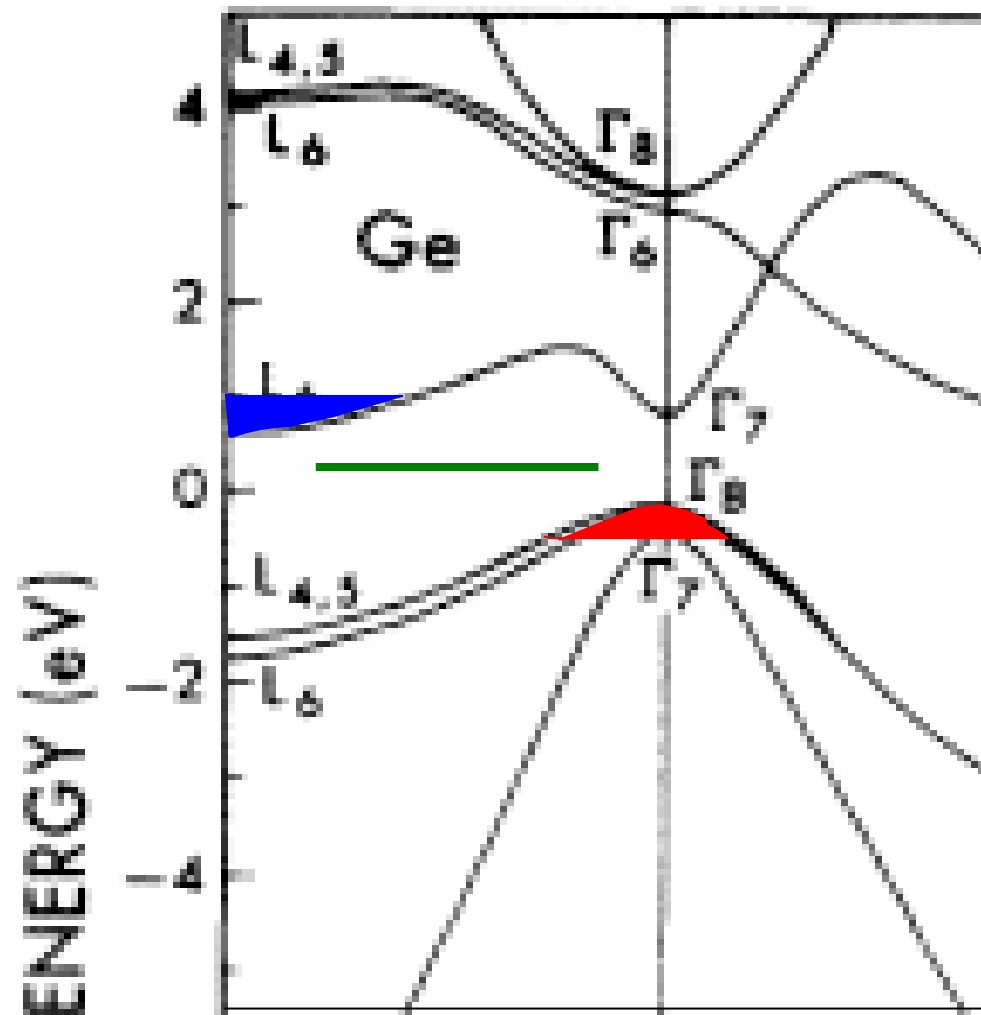


- Deep level *impurities*: e.g., Au and Fe in Si, transition metals, Cu in Ge, etc.
- *Native defects*: vacancies, interstitials, antisites in compound semiconductors (As on Ga sites: As_{Ga}); the concentration of antisites is strongly affected by stoichiometry (e.g., SI GaAs has $10^{16} \text{ cm}^{-3} \text{ As}_{\text{Ga}}$).

Deep levels are localized in real space but extended in k-space. Their binding energies $E \gg 3/2kT$. The capture cross sections vary between 10^{-12} and 10^{-26} cm^2 .



Deep Level in k-Space





Electric Charge Transport



At low electric fields the carrier velocity \vec{v} is proportional to the electric field \vec{E} :

$$\vec{v} = \mu \vec{E}$$

The mobility μ rises with decreasing temperature:

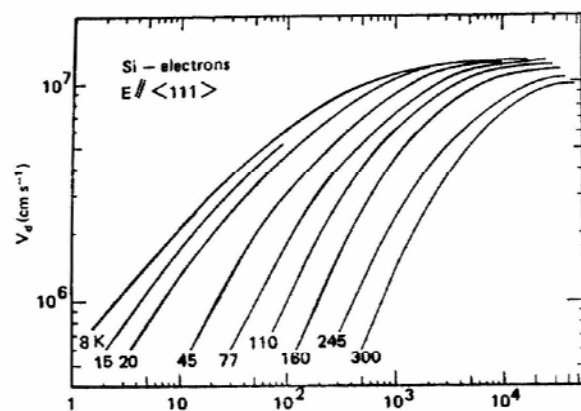
	electrons	holes	temp (K)
$\mu_{\text{Si}}:$			
(cm ² /Vs)	21,000	11,000	77
	1,350	480	300
$\mu_{\text{Ge}}:$			
(cm ² /Vs)	40,000	40,000	77
	3,900	1,900	300

At high electric fields velocity saturation occurs. The carriers emit phonons* at a rapidly increasing rate and the velocity becomes almost constant. It is interesting to note that the saturation velocity for most semiconductors lies around 10^7 cm/s.

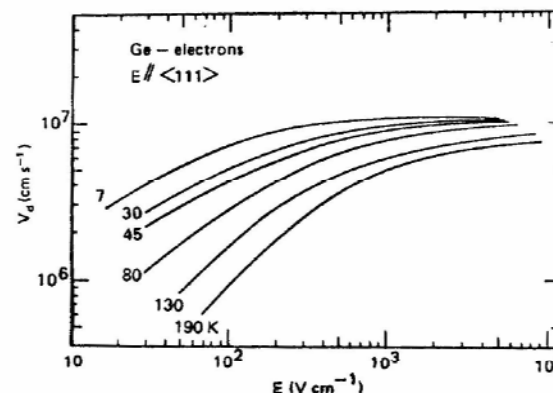
* Lattice vibrations (quantized $E = \hbar\omega$)



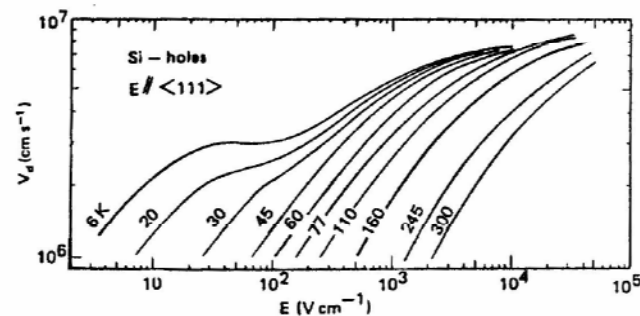
Free Carrier Velocity as a Function of the Electric Field



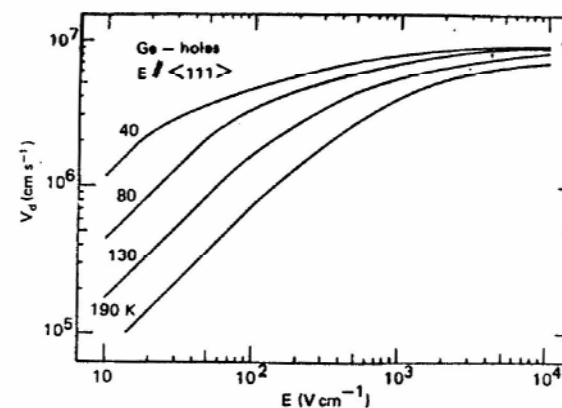
(a)



(c)



(b)



(d)

Drift velocity as a function of electric field applied parallel to the $\langle 111 \rangle$ crystallographic direction. Absolute temperature is the parameter for the different curves. (a) Electrons in silicon; (b) holes in silicon; (c) electrons in germanium; (d) holes in germanium.

Courtesy of G. Ottaviani, C. Canali, and A. Alberigi Quaranta, IEEE Trans. Nucl. Sci. NS-22 (1), 192 (1975).



The $\mu\tau$ Product

- Mobility μ : $v = \mu E$
- Carrier lifetime τ : Average time a minority carrier lives
- Distance d a carrier travels: $d = \mu \tau E$
- d should be much larger than the inter-contact distance



Semiconductor Properties

Compilation of the physical properties of compound semiconductors for which spectroscopic results have been reported, grouped according to density

Parameter	Si	4H-SiC	InP	GaAs	Ge	Cd _{0.35} Mn _{0.55} Te	Cd _{0.7} Zn _{0.3} Se	Cd _{0.9} Zn _{0.1} Te	CdSe	CdTe	PbI ₂	HgI ₂	TlBr
Density (g cm ⁻³)	2.33	3.21	4.78	5.32	5.33	5.8	5.5	5.78	5.81	5.85	6.2	6.4	7.56
Average atomic number(s)	14	10	32	31.5	32	49	38	49.1	41	50	63	62	58
Band gap (eV)	1.12	3.26	1.35	1.43	0.67	1.73	2.0	1.572	1.73	1.44	2.32	2.15	2.68
Pair creation energy (eV)	3.62	7.8	4.2	4.2	2.96	2.12	6.0	4.64	5.5	4.43	4.9	4.2	6.5
Electron mobility (cm ² V ⁻¹ s)	1400	1000	4600	8000	3900			1000	840	1100	8	100	30
Hole mobility (cm ² V ⁻¹ s)	1900	115	150	400	1900		10	120	75	100	2	4	4
Electron lifetime (s)	> 10 ⁻³	5 × 10 ⁻⁷	1.5 × 10 ⁻⁹	10 ⁻⁸	> 10 ⁻³			3 × 10 ⁻⁶	10 ⁻⁷	3 × 10 ⁻⁶	10 ⁻⁶	3 × 10 ⁻⁶	2.5 × 10 ⁻⁶
Hole lifetime (s)	10 ⁻³	7 × 10 ⁻⁷	< 10 ⁻⁷	10 ⁻⁷	2 × 10 ⁻³	10 ⁻⁷	10 ⁻⁷	1 × 10 ⁻⁶	10 ⁻⁶	2 × 10 ⁻⁶	3 × 10 ⁻⁷	1 × 10 ⁻⁵	3.7 × 10 ⁻⁵
Electron $\mu\tau$ product (cm ² V ⁻¹)	> 1	4 × 10 ⁻⁴	5 × 10 ⁻⁶	8 × 10 ⁻⁵	> 1	> 10 ⁻⁶	~ 10 ⁻⁴	4 × 10 ⁻³	6.3 × 10 ⁻⁵	3 × 10 ⁻³	1 × 10 ⁻⁵	3 × 10 ⁻⁴	5 × 10 ⁻⁴
Hole $\mu\tau$ product (cm ² V ⁻¹)	~ 1	8 × 10 ⁻⁵	< 1.5 × 10 ⁻⁵	4 × 10 ⁻⁶	> 1		10 ⁻⁶	1.2 × 10 ⁻⁴	7.5 × 10 ⁻⁵	2 × 10 ⁻⁴	3 × 10 ⁻⁷	4 × 10 ⁻⁵	2 × 10 ⁻⁶
Crystal structure	Cubic	Hexagonal	Cubic (ZB)	Cubic (ZB)	Cubic	Hexagonal	Hexagonal	Cubic (ZB)	Wurtzite	Cubic (ZB)	Hexagonal	Tetragonal	Cubic (CsCl)
Lattice constant (Å)	5.4309	53.079 (a)	5.048 (c)	5.8686	5.6533	5.64613			4.2999 (a)	7.0109 (c)	6.48	4.37 (a)	12.44 (c)
Knoop hardness (kg mm ⁻²)	1150	2540	460	750	692			?	90–130	60	< 10	< 10	12
Melting point (°C)	1412	2827	1060	1238	958	1080	1320	1092–1295	1239	1092	408	259	460
Dielectric constant	11.7	9.7	12.4	12.8	16			10	10.2	10.9		8.8	29.8
Resistivity (Ω/cm)	< 10 ⁴	> 10 ⁵	10 ⁶	10 ⁷	50	10 ¹⁰	10 ¹⁰	3 × 10 ¹⁰	10 ⁹	10 ⁹	10 ¹³	10 ¹³	10 ¹²
1/e abs. Depth (mm) at 10 keV	0.127	0.128	0.020	0.051	0.050	0.019	0.019	0.011	0.019	0.011	0.011	0.011	0.011
at 100 keV	23.30	17.90	1.597	3.46	3.51	1.5	1.5	1.01	1.5	1.01	0.453	0.46	0.32
Typ. FWHM ΔE (keV) at 60 keV	0.4	2.7	12	0.7	0.3	21	1.8	1.5	8.5	1.1	1.83	3.5	7.9
Intrinsic. FWHM ΔE (keV) at 60 keV (Fano noise)	0.415	0.642	0.443	0.439	0.250	0.530	0.530	0.393	0.506	0.300	0.441	0.409	0.550
Typical thickness (mm)	0.3	0.3	0.2	0.2	20	0.5	0.1	2	0.5	2	0.1	10	1

Note: For comparison, the properties of the elemental semiconductors, Si and Ge are also listed. The Fano noise was calculated using the “best” reported values of the Fano factor, otherwise a value of 0.14 was assumed.

A. Owen, A. Peacock / Nuclear Instruments and Methods in Physics Research A 531 (2004) 18–37



Interaction of Radiation with Semiconductors



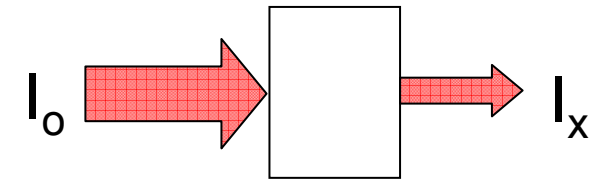
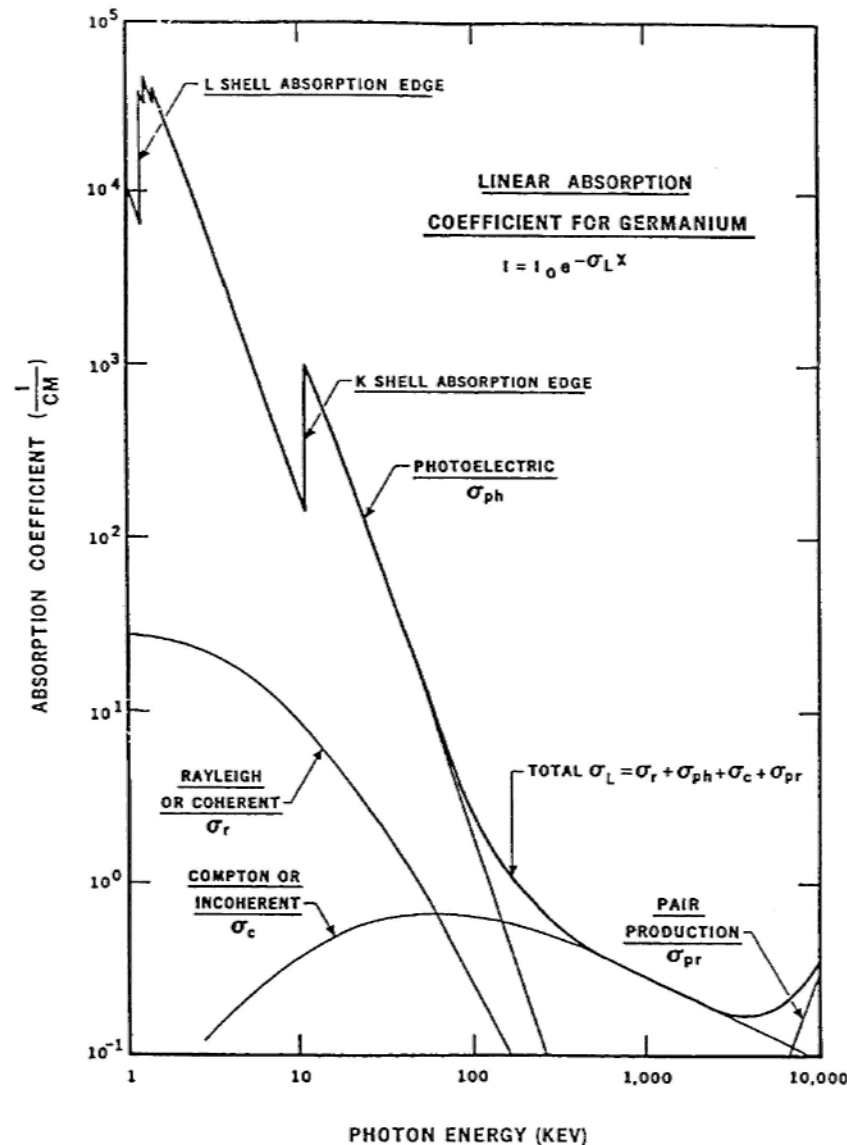
photons: - photo effect
- Compton effect
- pair production ($E > 2m_e c^2$)

} energetic electrons
→ e/h pairs

particles: - ionization → e/h pairs



Photon Absorption in Ge



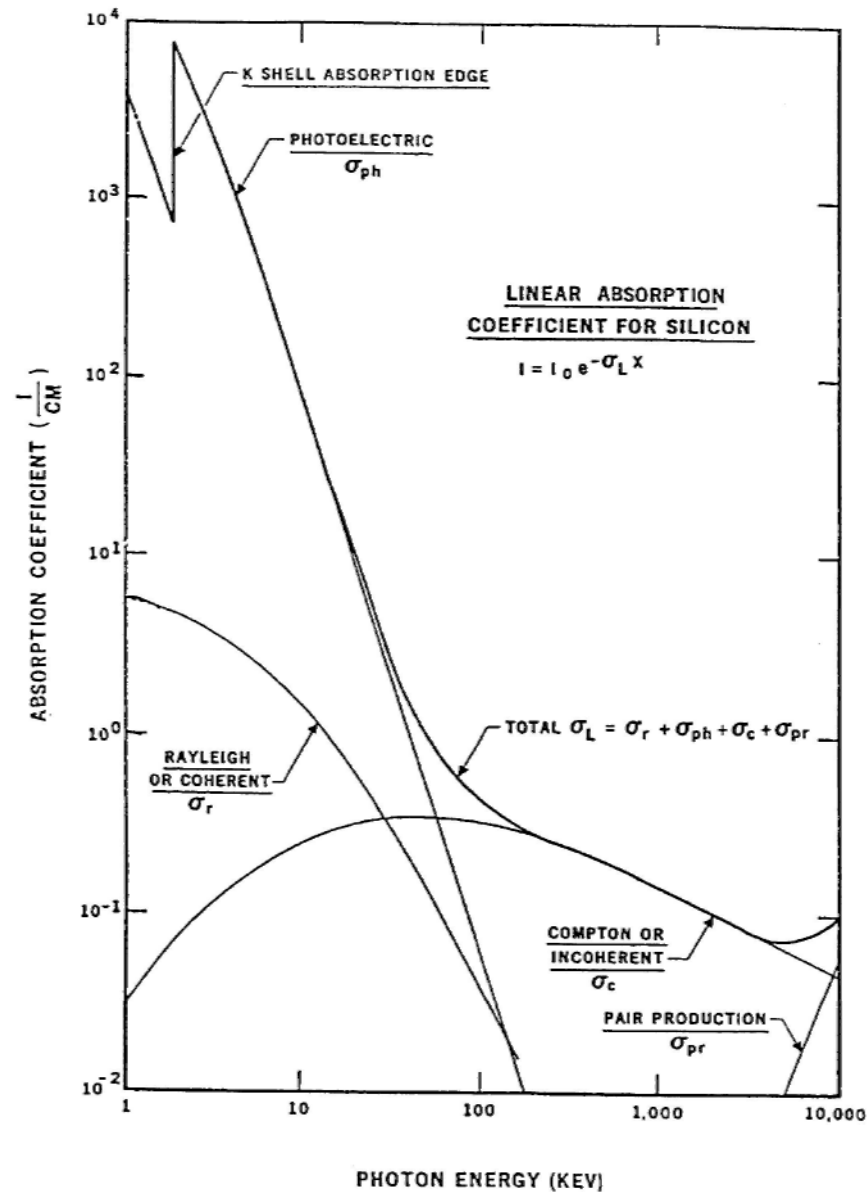
Absorber
Si, Ge, etc.

$$I_x = I_0 \exp(-\alpha x)$$

α = linear absorption
coefficient



Photon Absorption in Si



2/15/2006

E. E. Haller 29

XBL 791-8040



Requirements for the Ideal Solid State Ionization Chamber

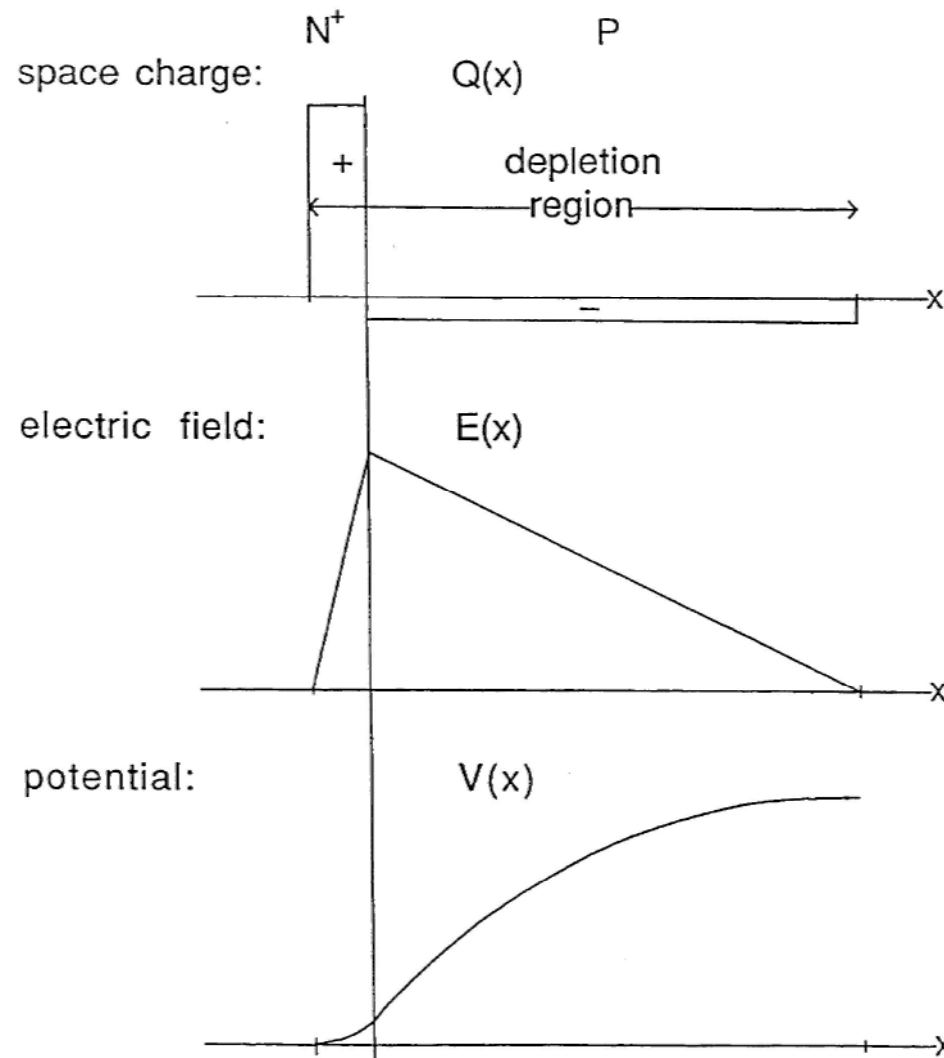
- excellent charge transport (no trapping, complete collection)
- no free mobile charges in the absence of radiation (i.e., low leakage current)
- linearity between the energy of the incident radiation and the number of e/h pairs
- maximum number of e/h pairs per unit energy
- high detection efficiency (large Z, large volume)
- short charge collection time (fast timing)
- convenient operating temperature
- position information (for some applications)
- inexpensive



P-N and P-I-N Junctions



The Asymmetric Planar N⁺-P-Junction (parallel plate capacitor)





Planar N⁺-P-Junction



The ionized shallow impurity levels constitute a space charge $e |N_A - N_D|$. Poisson's equation relates the potential ϕ to the charge:

$$\nabla^2 \phi = -e |N_A - N_D| / \epsilon \epsilon_0$$

ϵ = dielectric constant, ϵ_0 = permittivity of vacuum

In one dimension:

$$\partial^2 \phi / \partial x^2 = -e |N_A - N_D| / \epsilon \epsilon_0$$

integrating twice leads to:

$$\phi = d^2 |N_A - N_D| \frac{e}{2\epsilon \epsilon_0} = d^2 |N_A - N_D| C$$

$$C_{Si} = 7.72 \times 10^{-8} \text{ Vcm}$$

$$C_{Ge} = 5.64 \times 10^{-8} \text{ Vcm}$$

with:

d = width of the depletion layer



Planar N⁺-P-Junction



For Ge junctions we find:

$$V = d^2 | N_A - N_D | \times 5.64 \times 10^{-8} \text{ (Vcm)}$$

and for Si:

$$V = d^2 | N_A - N_D | \times 7.72 \times 10^{-8} \text{ (Vcm)}$$

with

V = applied voltage (V)

d = depletion depth (cm)

$| N_A - N_D |$ = net-impurity concentration (cm⁻³)

EXAMPLE: Planar P-I-N Detector

$$d = 2 \text{ cm}, V = 3000\text{V}$$

What has $| N_A - N_D |$ to be for full depletion?

$$\text{Ge: } 1.33 \times 10^{10} \text{ cm}^{-3}$$

$$\text{Si: } 9.7 \times 10^9 \text{ cm}^{-3}$$



*These are extremely small concentrations
compared to $\sim 4 \times 10^{22}$ Ge or Si per cm³!*



Ultra-Pure Semiconductors

Motivation:

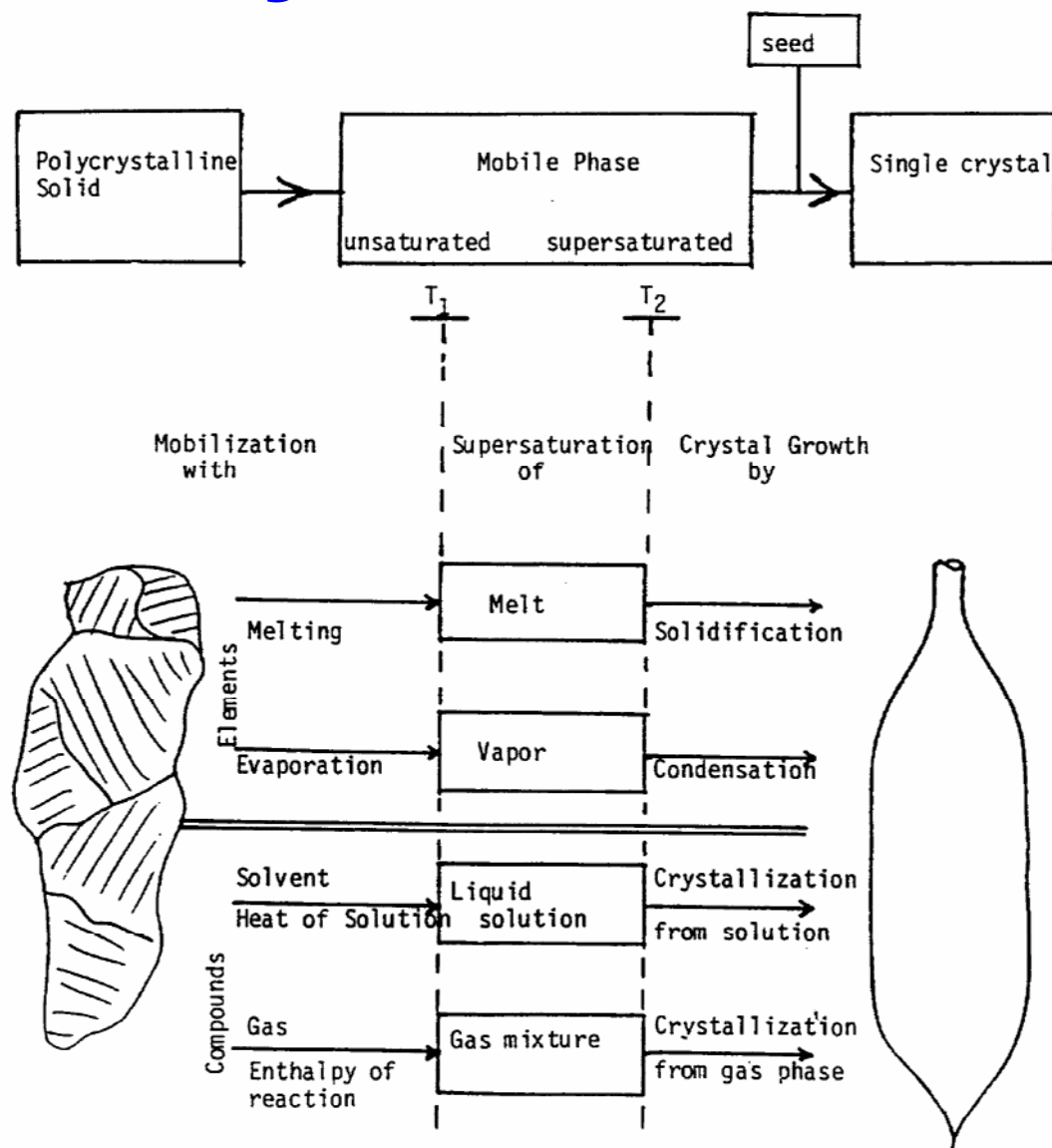
- Large depletion layers
- Low defect concentrations -> large lifetimes

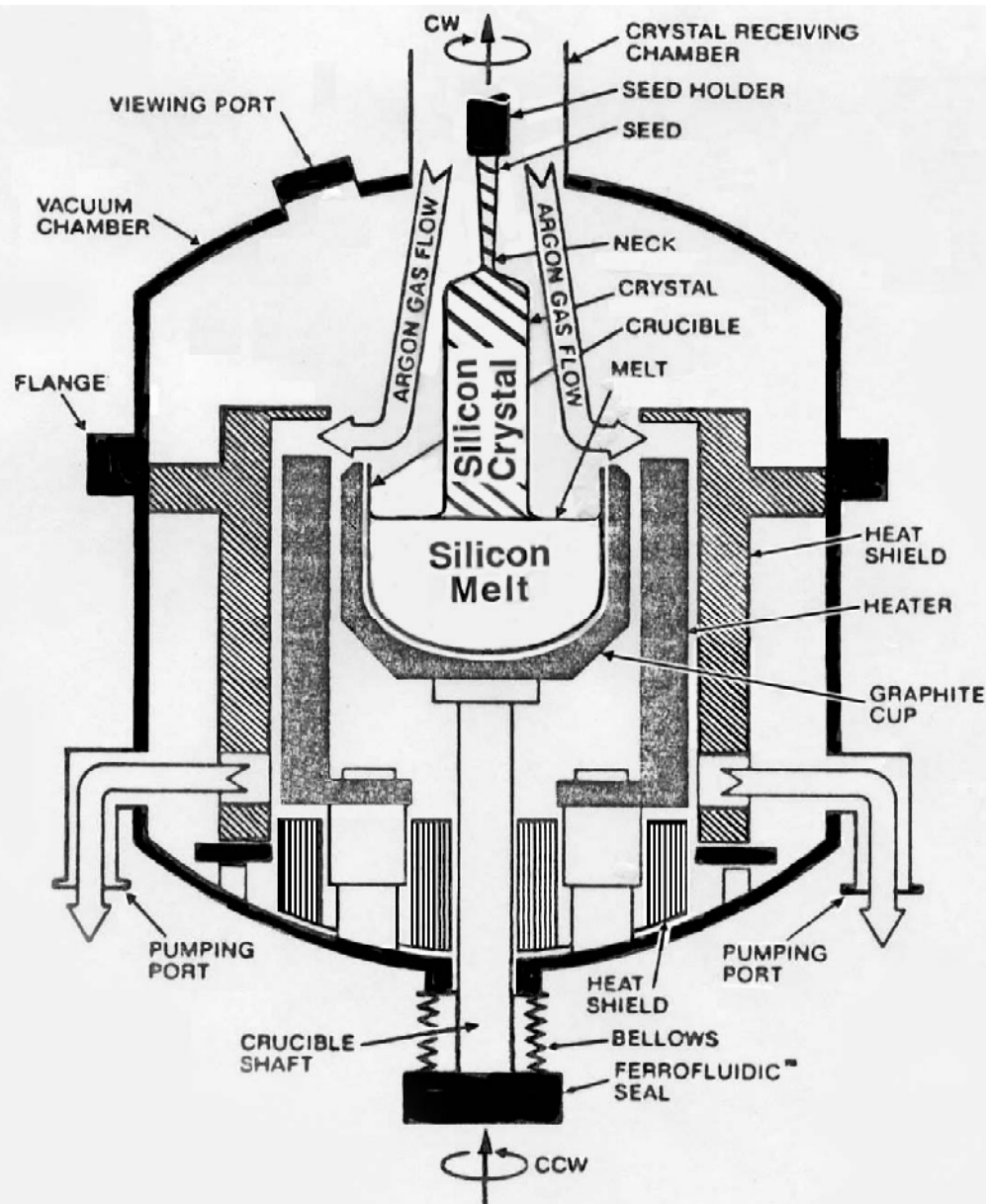
Approach:

- Ultra-pure Ge grown from a synthetic silica crucible in 1 atm. of pure H_2
- Floating-Zone (FZ) Si grown in vacuum
- Liquid Phase Epitaxial GaAs



Crystal Growth





Jan Czochralski

Sketch of a Modern CZ-puller



Czochralski (CZ)
Silicon single
crystal;

8 inches (20 cm)
in diameter and
over 6 feet (~2
m) long;

Weight ~ 320 lb
(145 kg)

2/15/2006

E. E. Haller 38



15

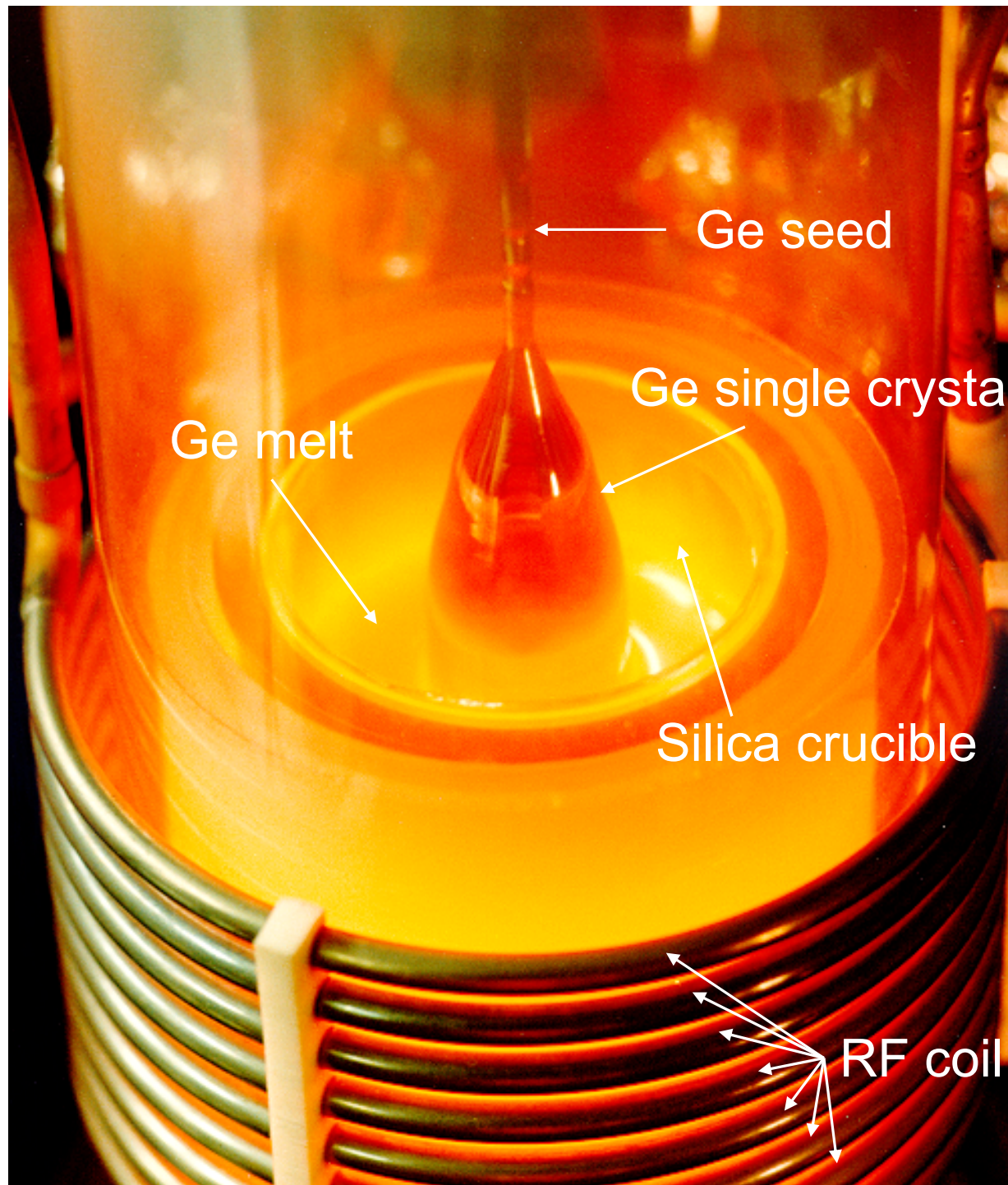


HOCHTECHNOLOGIE: EIN 300-MM-STAB AUS DER HIKARI-PRODUKTION.

Modern Silicon single crystal grown by the Czochralski technique at the Wacker Silitronix Hikari plant in Japan. The diameter is 12 inches (300 mm) and the length is over 4 feet.

2/15/2006

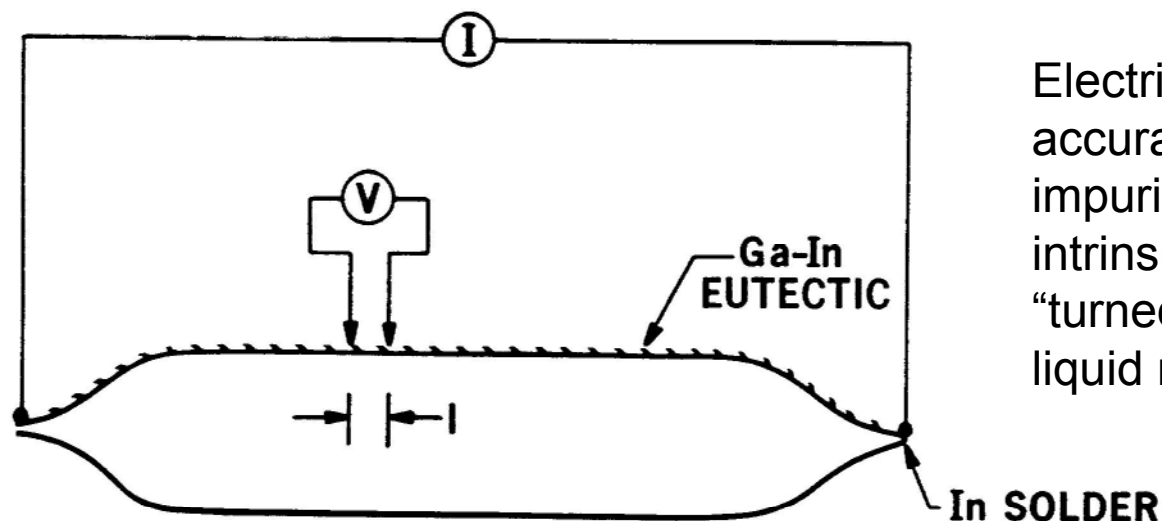
E. E. Haller 39



An ultra-pure Germanium single crystal is being “pulled” from a melt contained in a silica crucible at 936°C. The atmosphere is pure Hydrogen. Heat is supplied by the water cooled radiofrequency (RF) coil surrounding the silica envelope. This bulk crystal growth technique carries the name of it’s inventor, “Jan Czochralski.”



Determining Ultra-Purity



Electrical conductivity is an accurate measure of the net-impurity concentration. The intrinsic conduction can be “turned-off” through cooling to liquid nitrogen temperature (77K).

$$\rho = \frac{V}{I} \frac{A}{l} = \frac{1}{|N_A - N_D| e \mu}$$

$$|N_A - N_D| = \frac{I}{e \mu V} \frac{l}{A}$$

I: injected current

V: voltage drop across segment of length l

e: charge of electron
(1.6×10^{-19} As)

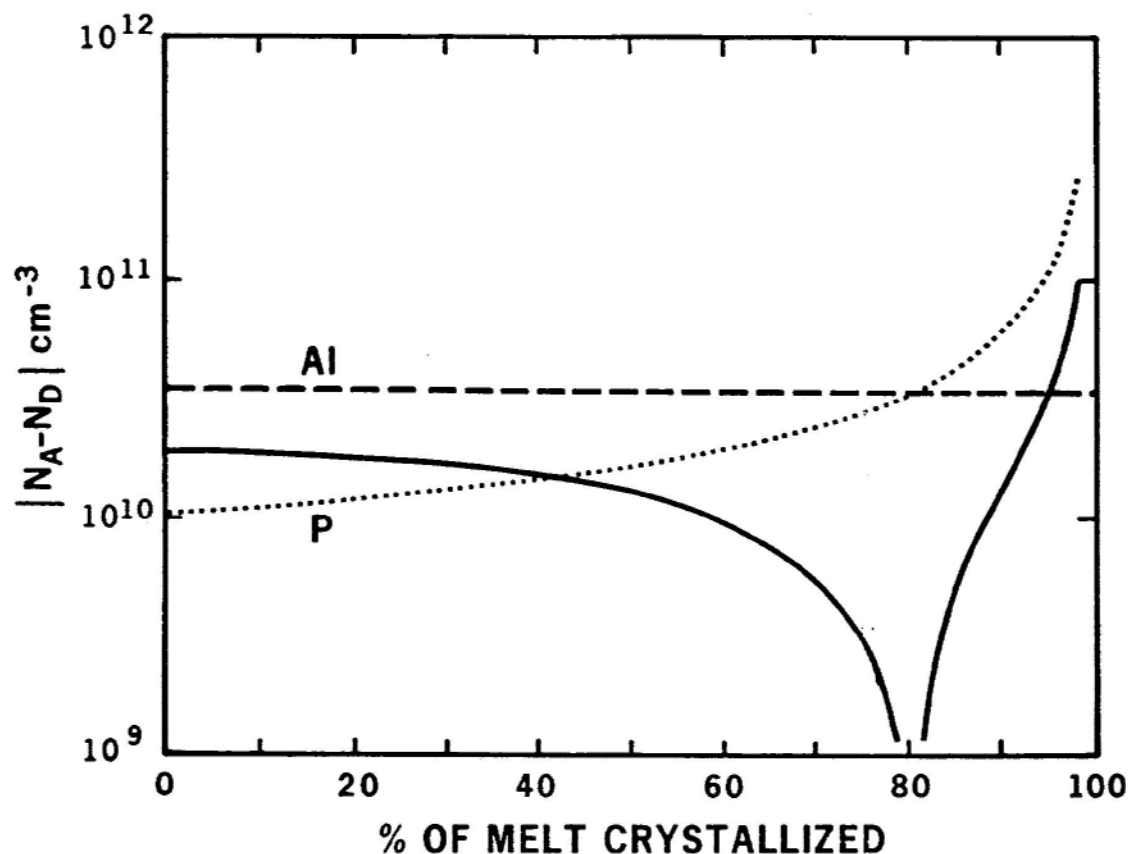
μ : mobility (equal for e & h at 77K)

A: cross sectional area

XBL 8210-3054



Dopant Impurity Profiles



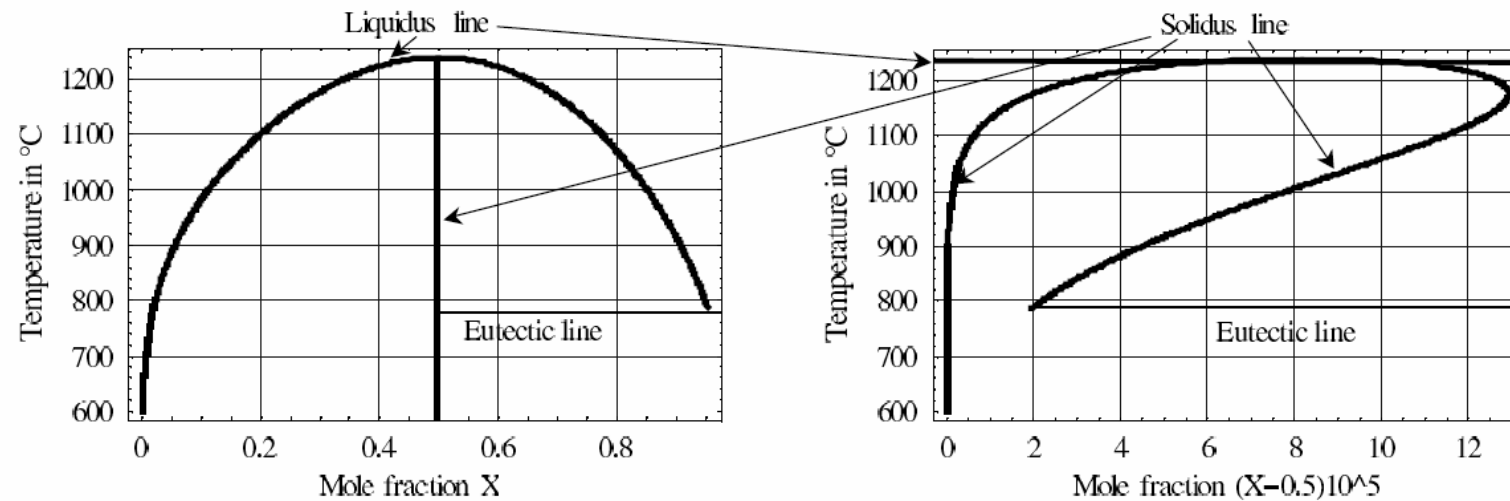
a)

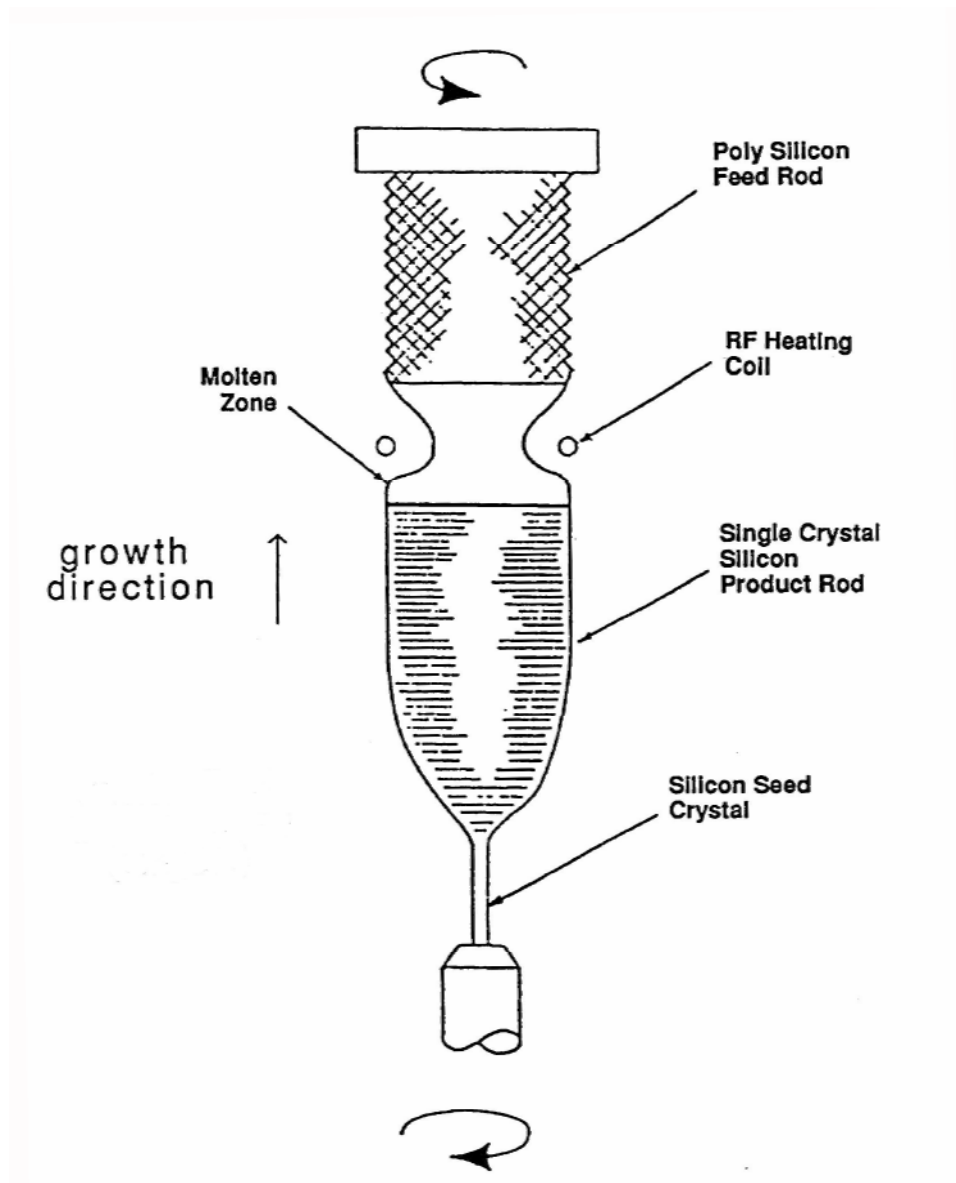
XBL 8210-3056

Typical impurity profile of an ultra-pure Ge crystal. The acceptor aluminum (Al, dashed line) does not segregate in silica grown Ge, leading to a constant concentration. The donor phosphorus segregates (P, dotted line). In our particular example, the phosphorus concentration equals the aluminum concentration at 80% of the melt frozen and exceeds it beyond. In the Al dominated part, the crystal is p-type, in the P dominated type, the crystal is n-type.

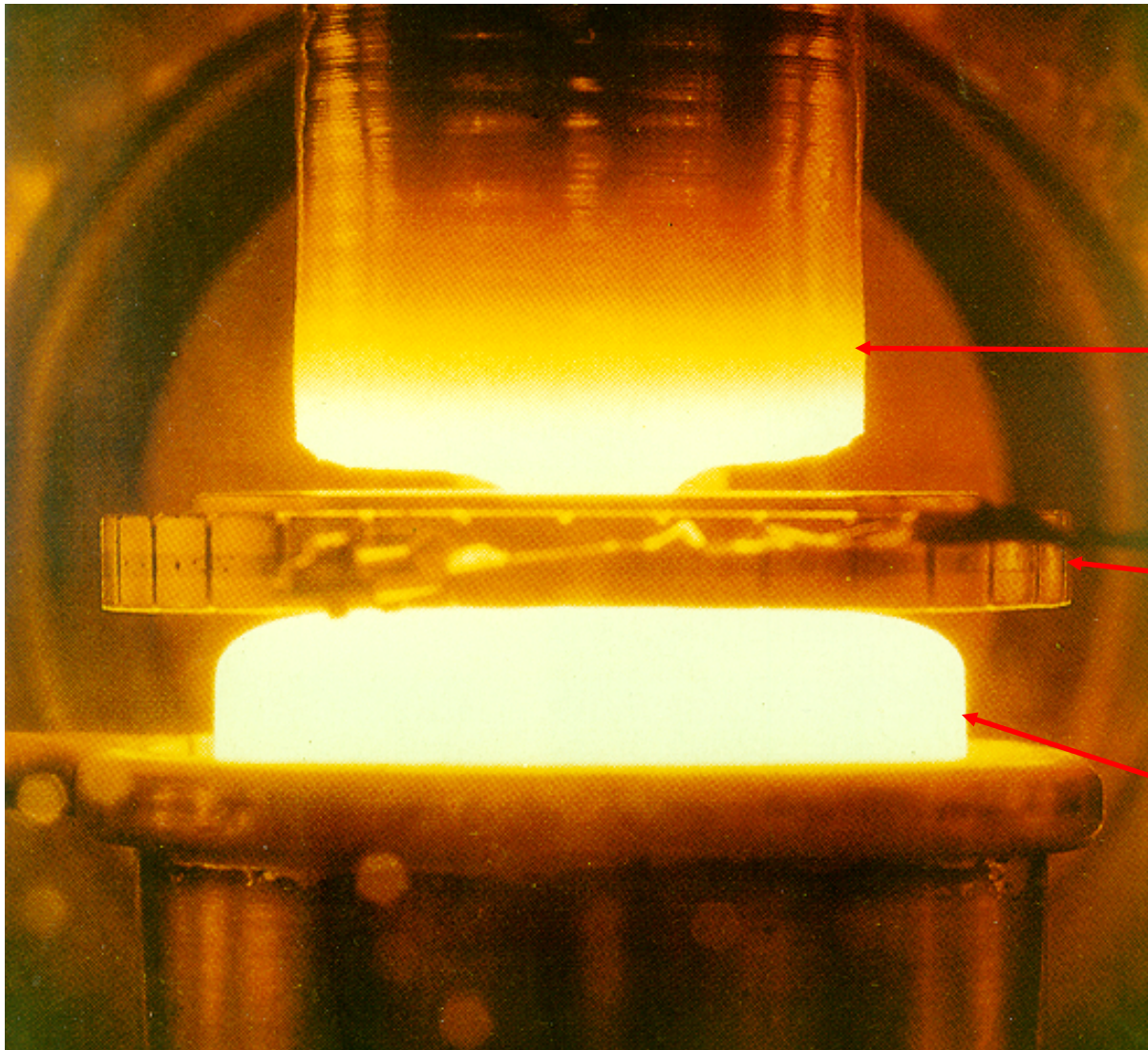


GaAs Phase Diagram





The **Floating Zone (FZ)** crystal growth process is used for ultra pure silicon up to 6" in diameter. No crucible is used. The ambient is typically nitrogen but vacuum and argon have been used.



Poly Si
feed rod

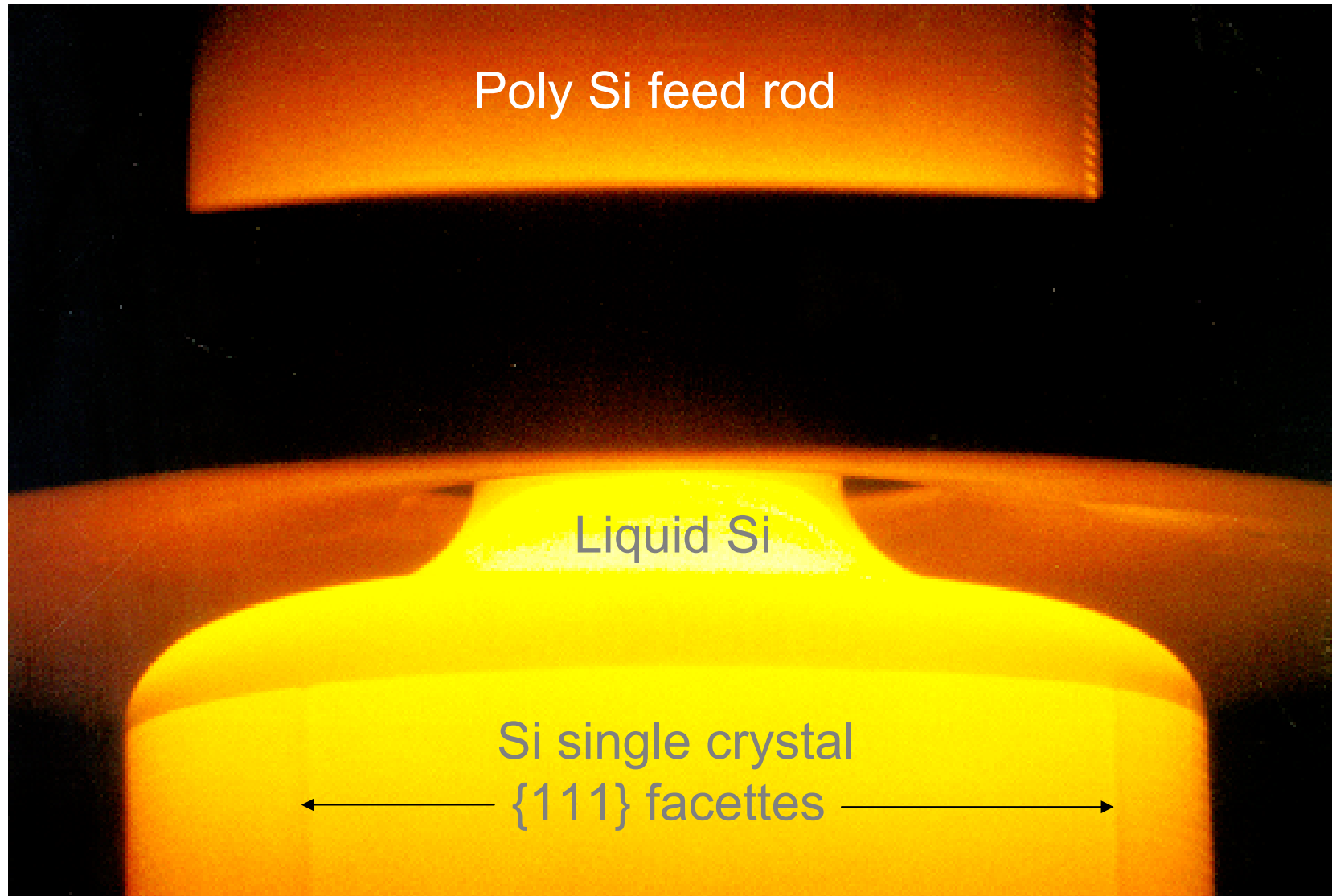
One
turn RF
coil

Si single
crystal

Silicon Floating Zone (FZ) crystal with 10 cm diameter is being pulled. The single turn RF heating coil creates the liquid “floating zone” between the lower part (single crystal) and the upper polycrystalline section.

2/15/2006

E. E. Haller 45

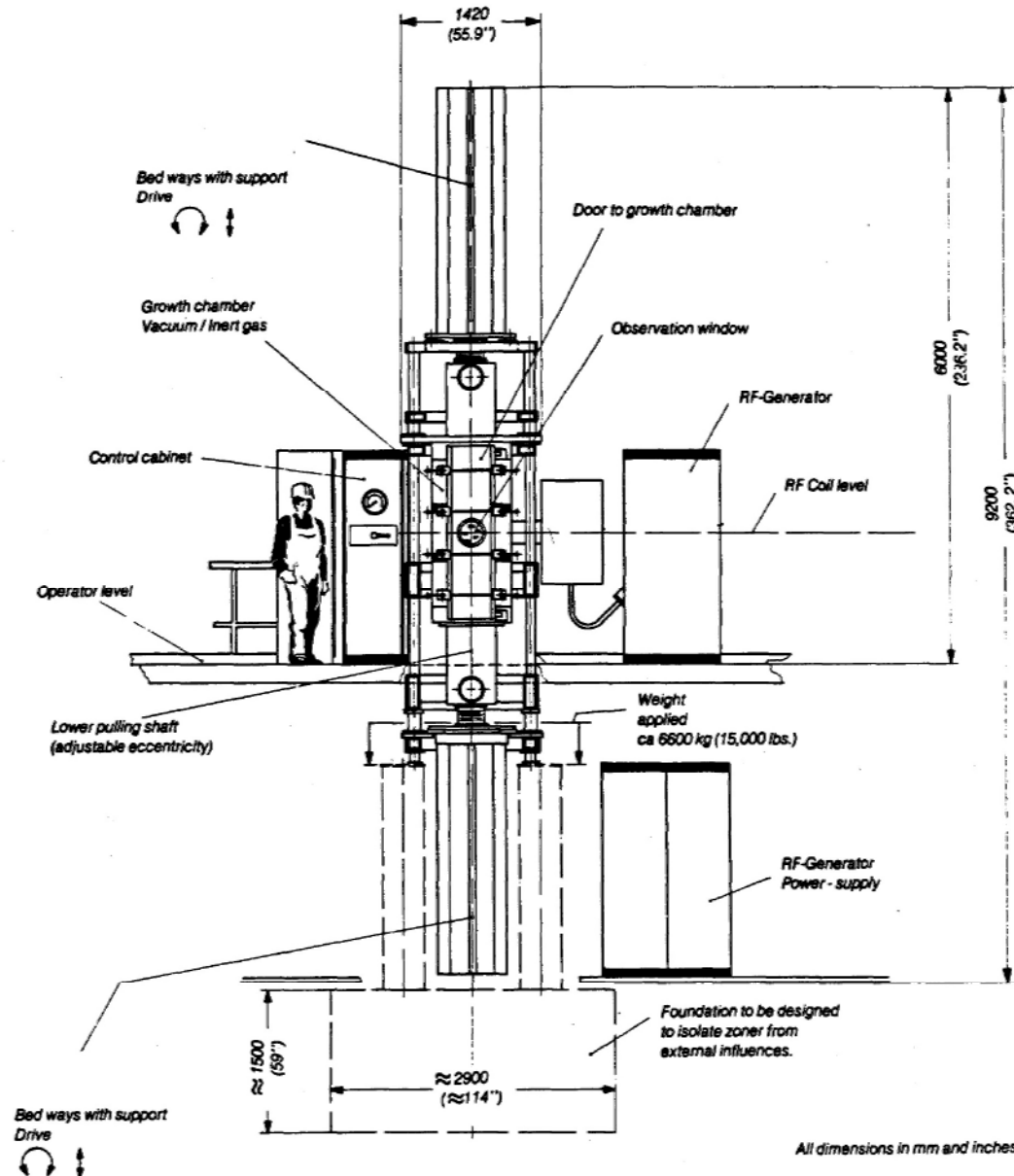


2/15/2006

E. E. Haller 46



Major Dimensions of Zoner VZA9

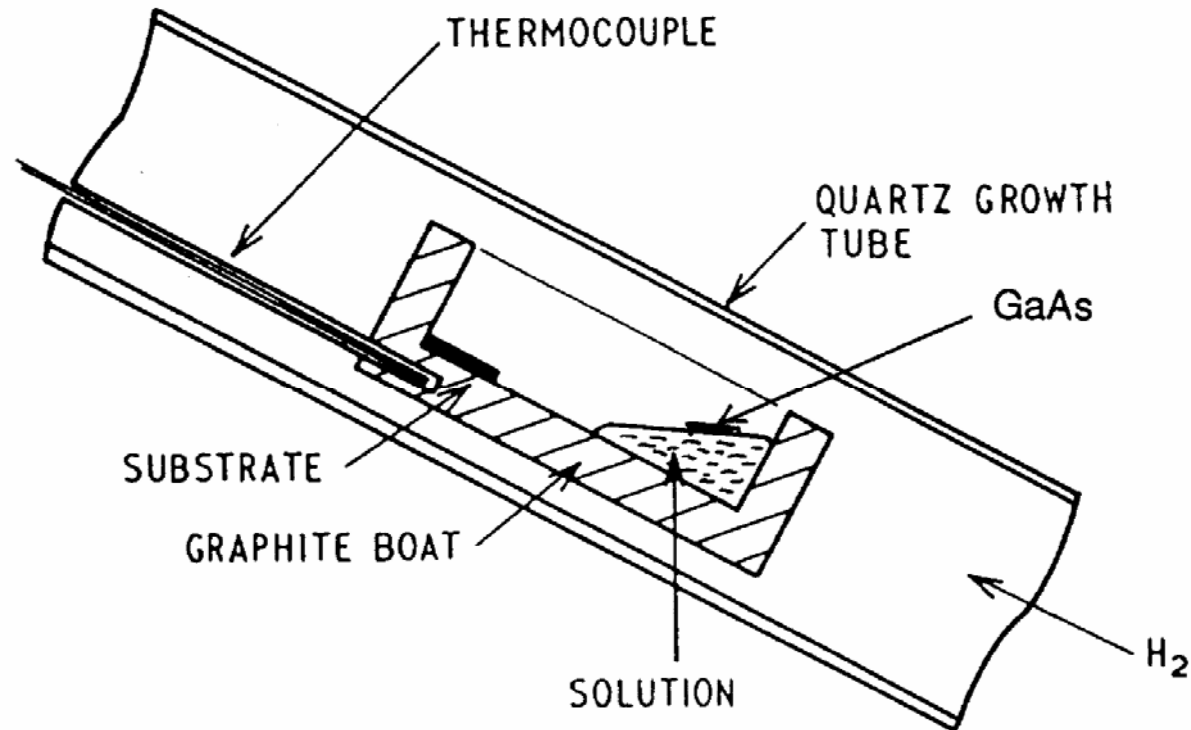


2/15/2006

E. E. Haller 47

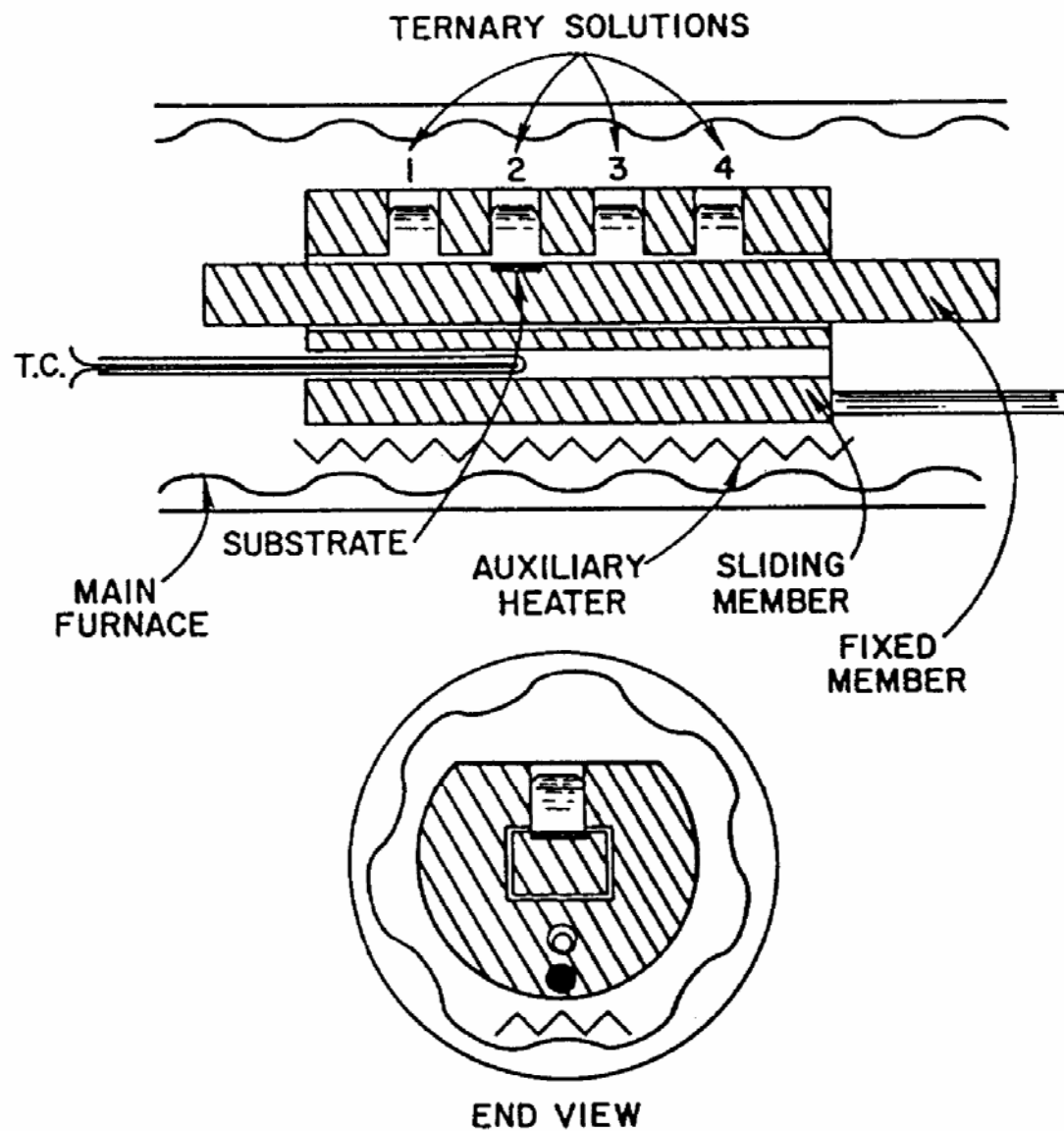


Liquid Phase Epitaxy LPE



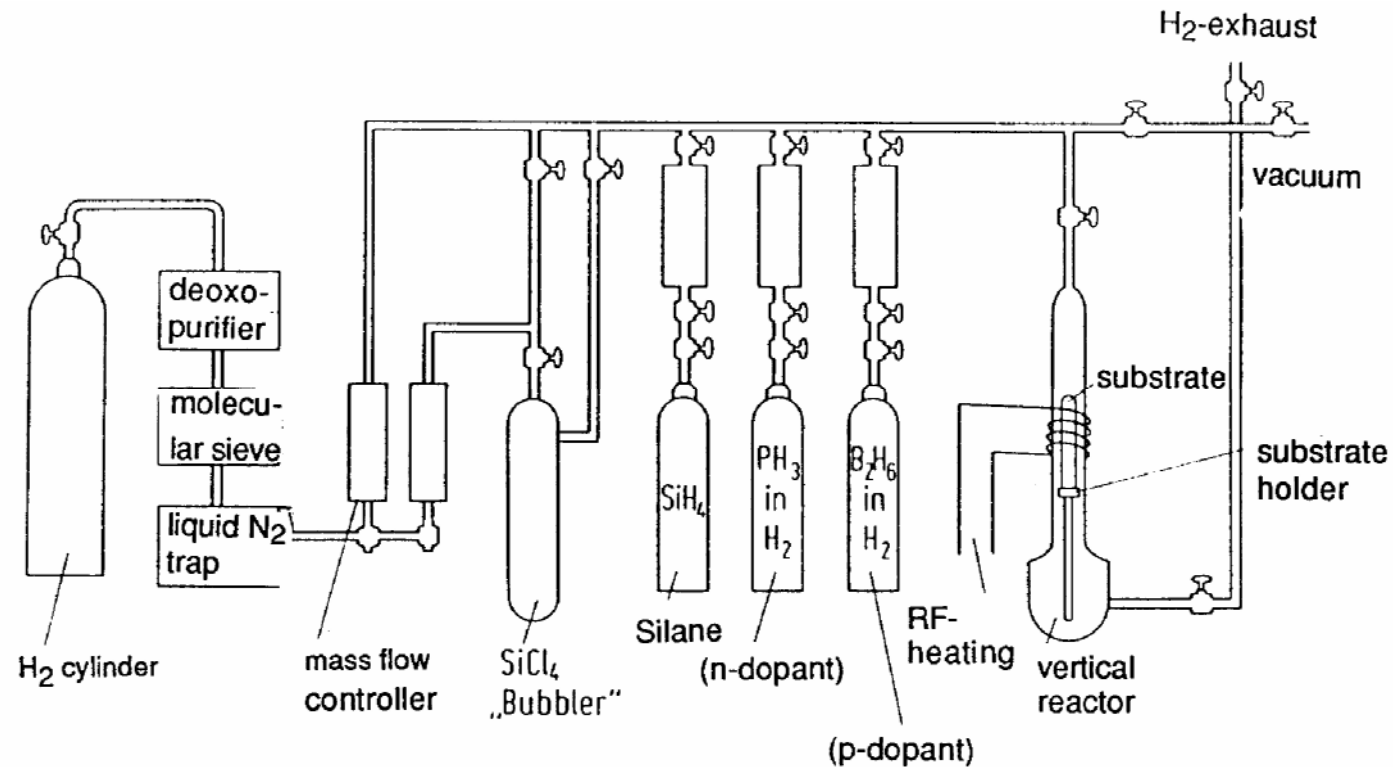


Multilayer LPE



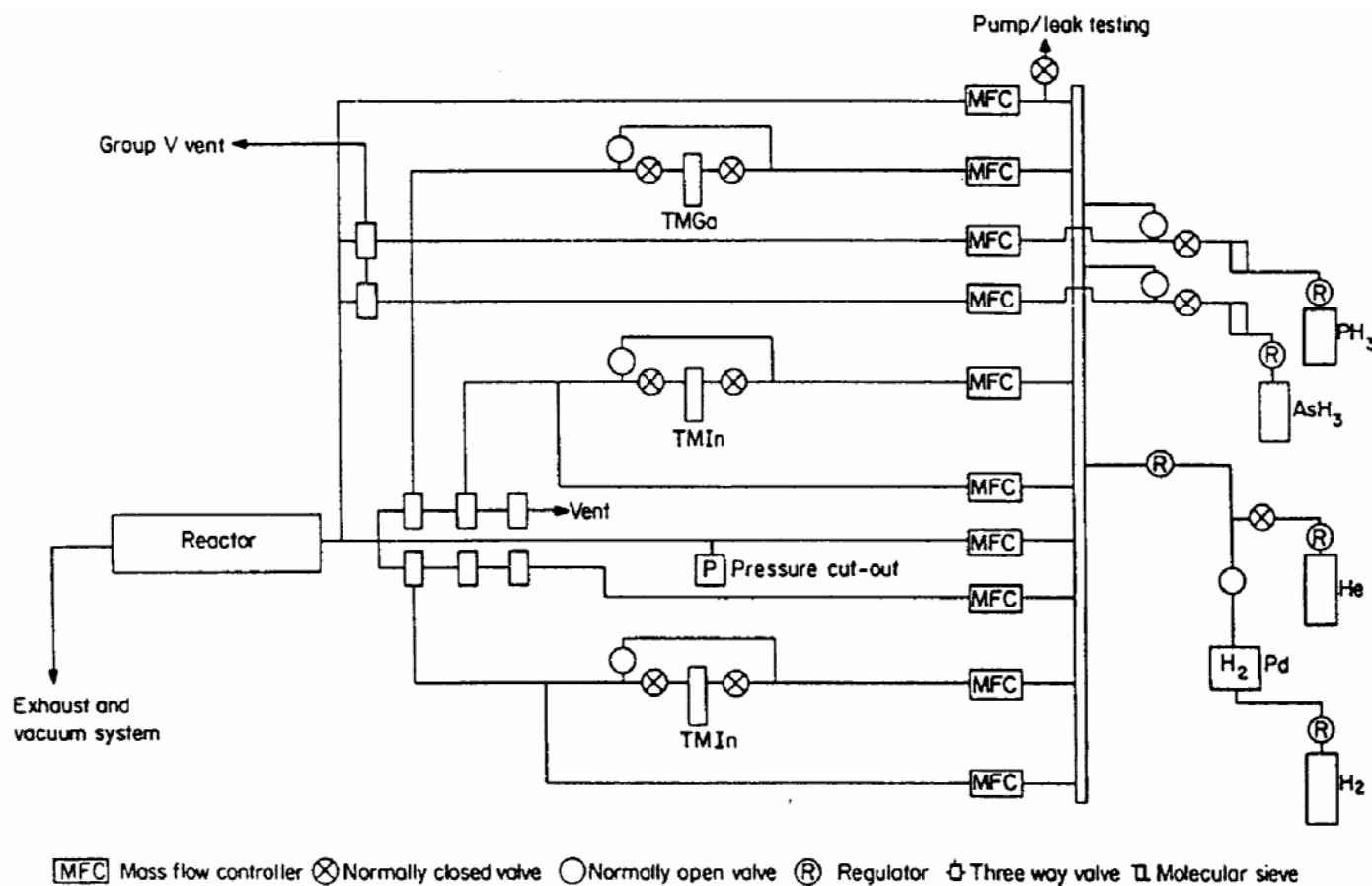


Chemical Vapor Deposition or Vapor Phase Epitaxy



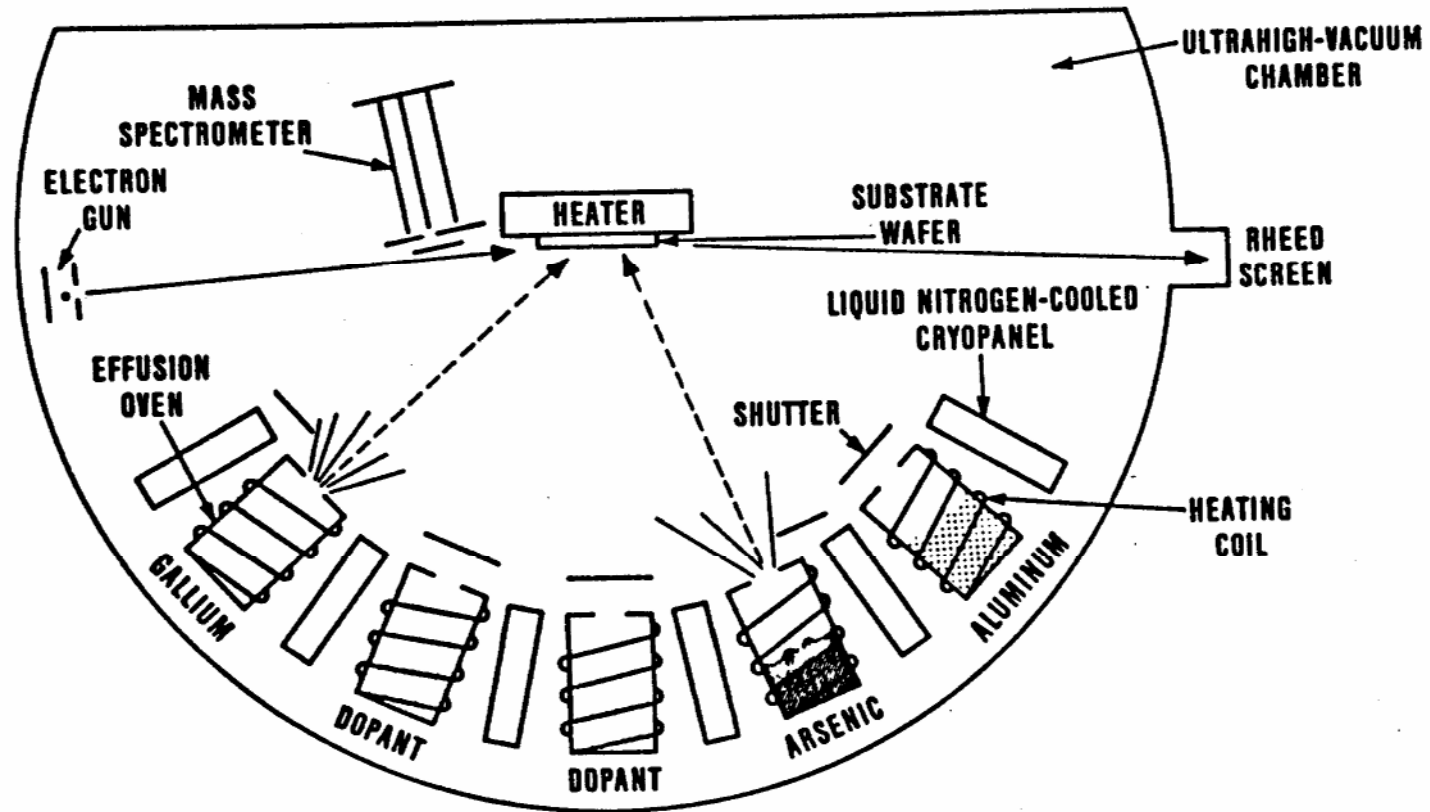


Metalorganic Chem.Vapor Deposition MOCVD





Molecular Beam Epitaxy MBE





High Bandgap-High Z Materials



- **Advantages:**

- no limitations imposed by cooling requirements (medical probes, etc.)
- small, efficient detection volume (medical probes, etc.)

- **Challenges:**

- crystal growth is difficult: low purity and poor structural perfection
- not all compound semiconductors can be doped p- and n-type
- trapping and polarization
- poor hole transport and short carrier lifetimes
- limited crystal size
- contact formation problems
- chemical stability



Properties of Compound Semiconductors



Material	Atomic Number	Density g/cm ³	Band gap (eV)	Knoop Hardness	E _{pair} (eV)	Resistivity Ω-cm	μ _τ (e) cm ² /V	μ _τ (h) cm ² /V
Si	14	2.33	1.12	1150	3.62	>10 ⁴	2.7x10 ⁻²	9.6x10 ⁻³
CdTe	48, 52	6.2	1.44	45	4.43	10 ⁹	3.5x10 ⁻³	2.3x10 ⁻⁴
CdZnTe	48, 30, 52	≈ 6	1.5 - 2.2		5.0 *	10 ¹¹	1x10 ⁻³	6x10 ⁻⁶
CdSe	48, 34	5.81	1.73		5.5**	10 ⁸	7.2x10 ⁻⁴	7.5x10 ⁻⁵
CdZnSe	48, 30, 34	≈ 5.5	1.7-2.7			3x10 ⁸	1x10 ⁻⁴	
HgI ₂	80, 53	6.4	2.13	<10	4.2	10 ¹³	1x10 ⁻⁴	4x10 ⁻⁵
TlBrI	81, 35, 53	7.5	2.2-2.8	40		10 ¹⁰	9x10 ⁻⁵	
GaAs	31, 33	5.32	1.43	750	4.2	10 ⁷	8x10 ⁻⁵	4x10 ⁻⁶
InI	49, 53	5.31	2.01	27		10 ¹¹	7x10 ⁻⁵	
GaSe	31, 34	4.55	2.03		4.5		3.5x10 ⁻⁵	9x10 ⁻⁶
diamond	6	3.51	5.4	10 ⁴	13.25		2x10 ⁻⁵	
TlBr	81, 35	7.56	2.68	12	6.5	10 ¹²	1.6x10 ⁻⁵	1.5x10 ⁻⁶
PbI ₂	82, 53	6.2	2.32	<10	4.9	10 ¹³	8x10 ⁻⁶	2x10 ⁻⁷
InP	49, 15	4.78	1.35	535	4.2	10 ⁷	4.8x10 ⁻⁶	< 1.5x10 ⁻⁵
ZnTe	30, 52	5.72	2.26		7.0 **	10 ¹⁰	1.4x10 ⁻⁶	7x10 ⁻⁵
HgBrI	80, 35, 53	6.2	2.4-3.4	14		5x10 ¹³	2x10 ⁻⁷	< 1x10 ⁻⁷
a-Si	14	2.3	1.8		4	10 ¹²	6.8x10 ⁻⁸	2x10 ⁻⁸
a-Se	34	4.3	2.3		7	10 ¹²	5x10 ⁻⁹	1.4x10 ⁻⁸
BP	5, 15	2.9	2.1	4700	6.5**			
GaP	31, 15	4.13	2.24		7.0**			
CdS	48, 16	4.82	2.5		7.8**			
SiC	14, 6	3.2	2.86		9.0**			
AlSb	13, 51	4.26	1.62		5.05			
PbO	82, 8	9.8	1.9		6.47			
ZnSe	30, 34	5.42	2.58		8.0**			

[Courtesy M.R. Squillante
et al., MRS Proc. Vol.
302, 326 (1993)]

2/15/2006

{Note: materials are listed in order of decreasing μ_τ (e) at room temperature.}

* estimated for 20% zinc

** estimated

E. E. Haller 54



Room Temperature and High Z Materials: CdTe, CdZnTe, HgI₂ and GaAs

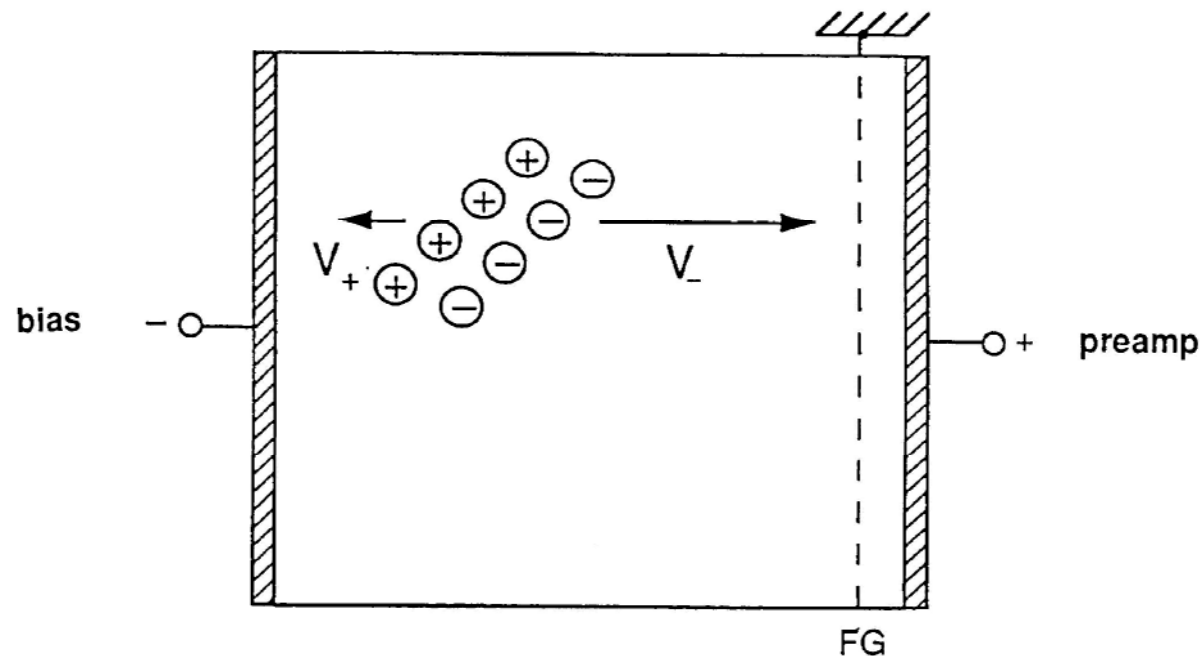
Major drivers for new detector materials development:

- room temperature operation ($E_{\text{gap}} > 1.4 \text{ eV}$)
- high efficiency (large Z)



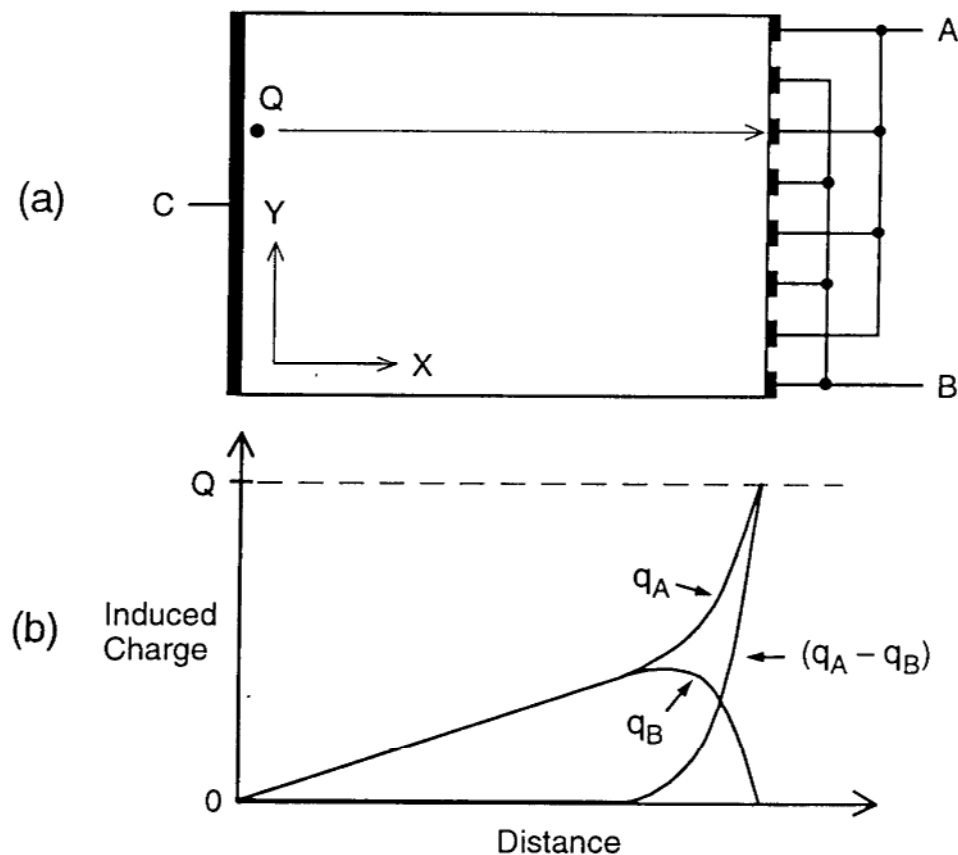
The “Frisch Grid”: An Old Idea with Great Relevance and Promise

- Gas ionization chambers suffer from the same problem as many semiconductor detectors: $\mu\tau$ of one charge species (ions) is significantly lower than of the other charge species (electrons).
- **Solution:** the "Frisch Grid" (FG)



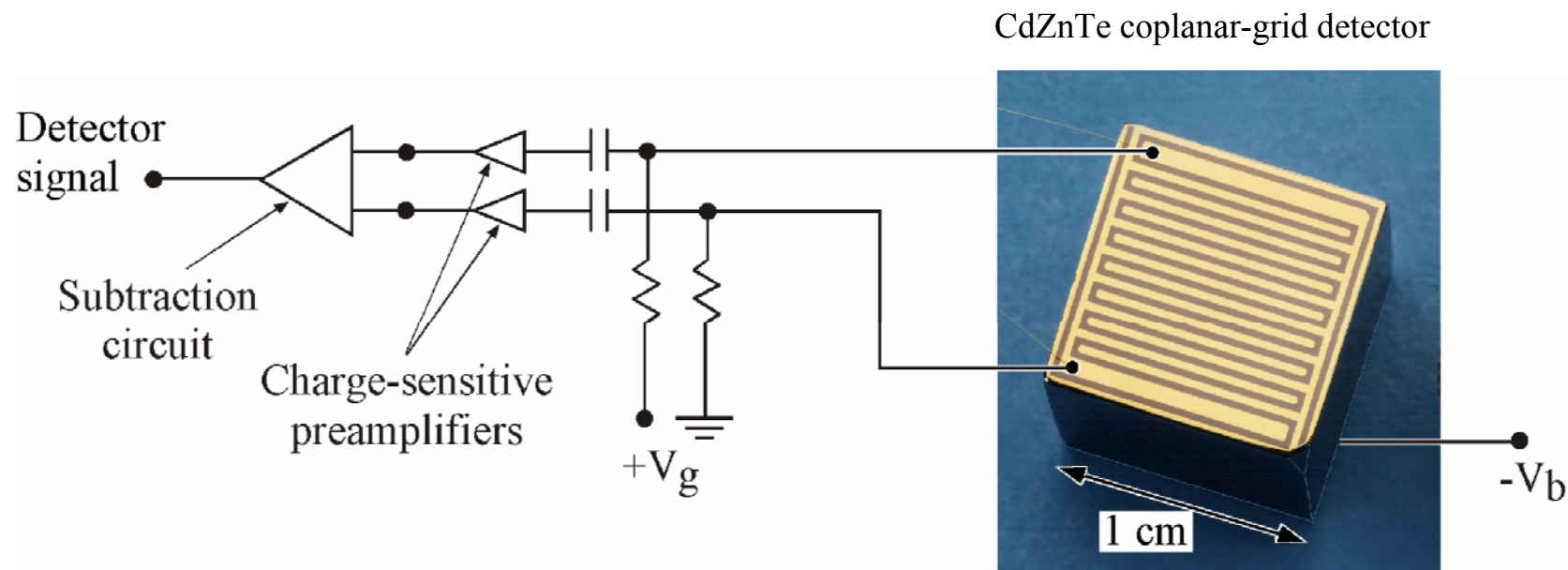


Reincarnation of the Frisch Grid as two sets of interdigitated contacts A and B





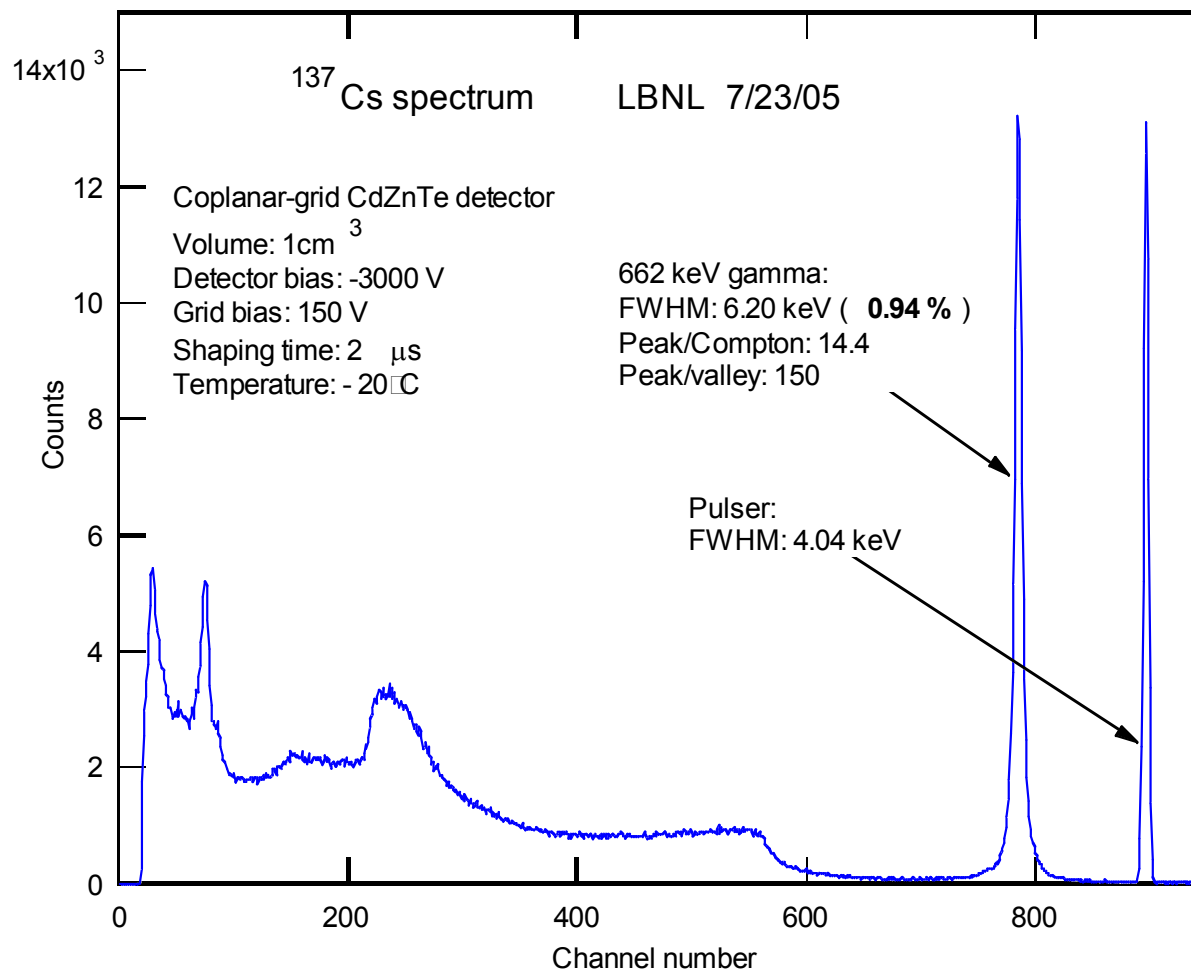
Operational Circuit for a Coplanar-Grid Detector



Courtesy P.N. Luke, LBNL



Recent Record



Courtesy P. N. Luke, LBNL



Conclusions



- The ideal semiconductor materials for all radiation detection applications does not exist but they can be approached closely.
- Certain material property requirements and application requirements are incompatible (e.g. bandgap: **large** for low leakage current but **small** for small energy per e/h pair).
- Si & Ge are the high resolution spectrometer materials. Detectors exhibit excellent stability, good efficiency, timing, etc.
- Thin epitaxial films (100-150 μm) of high-purity GaAs ($|N_A - N_D| < 10^{12} \text{ cm}^{-3}$) have been grown by the LPE technique and early spectrometer results look promising. In contrast, semi-insulating (SI) GaAs deliberately contains very large concentrations of deep traps which make the material highly resistive and lead to extreme charge trapping.



Conclusions, cont.



- CdTe, CdZnTe & HgI₂ are room temperature materials. Low energy X rays can be detected with good resolution. Medium and high energy photons (γ - rays) still pose problems (after over 40 years of R&D!). Trapping and poor hole transport seem to be fundamental and/or related to material inhomogeneities and defects.
- Single-polarity charge sensing using coplanar electrodes (an analog of the Frisch grid in gas proportional counters) looks very promising for semiconductors with good collection of at least one type of charge carrier (typically electrons; see: P.N. Luke, Appl. Phys. Lett. **65**, 2884 (1994) and more recent publications).
- The search for new semiconductor detector materials should remain realistic, balancing advantages and disadvantages (i.e., picking a good bandgap and a high Z is only part of the story!). The $\mu\tau$ product for electrons and for holes dominates charge collection.



3. Limitations of compound semiconductors

Unfortunately, compound semiconductors also suffer from several limitations, which do not affect their elemental counterparts. Perhaps the most severe of which is that one or both charge carriers suffer from poor transport—either through poor mobility or carrier lifetime. In this regard, the most useful figure of merit when comparing compounds is the mobility–lifetime product ($\mu\tau$). For the elemental semiconductors this is of the order of unity for both electrons and holes, whereas for compound semiconductors it rarely reaches greater than a few times 10^{-4} for electrons and 10^{-5} for holes—and these figures get worse with increasing Z . The cause can usually be traced to trapping centers caused by impurities, lack of stoichiometry, or for the softer materials, plastic deformation caused by mechanical damage during fabrication.

FACT

A. Dierker, A. Reussch / Nuclear Instruments and Methods in Physics Research A 531 (2004) 13–37



Thanks for your attention